TAMPERE UNIVERSITY OF TECHNOLOGY

TOMI NIHTILÄ

A SIMULATION TOOL FOR SYNCHRONIZATION OF MULTISTATIC RADAR

Master of Science Thesis

Examiners: Professor Karri Palovuori
and Professor Ari Visa.
Examiners and topic approved by the
Faculty Council of the Faculty of
Computing and Electrical Engineering
on 4 April 2012.

ABSTRACT

TAMPERE UNIVERSITY OF TECHNOLOGY
Master's Degree Programme in Electrical Engineering
NIHTILÄ, TOMI : A Simulation Tool for Synchronization of Multistatic Radar
Master of Science Thesis, 74 pages
June 2012
Major: Design of Electronic Circuits and Systems
Examiners: Professor Karri Palovuori and Professor Ari Visa
Keywords: radar simulation, synchronization of multistatic radar, pulsed Doppler radar, radar signals

Radar transmits electromagnetic waves and observes its surroundings by listening to the echoes reflected from objects. Conventional monostatic radar has a transmitter and receiver in the same system. The concept is commonly used and the implementation has many benefits. However, in military applications it is desired to make radar less visible, and a mean to achieve it is to spatially separate the transmitter and the electromagnetically invisible passive receiver. Multistatic radar has a transmitter and several separated receivers. This also allows the observation of targets from several angles which aids detecting targets using stealth techniques.

One of the challenges in implementing multistatic radar is the synchronization between transmitter and receiver which is needed for phase-coherent operation. Extreme stability in phase is required for the Doppler processing which is the basis of the efficient digital processing of modern radars. Instability weakens the radar performance, such as detection probability. Synchronization can be performed using a separate data link, optical fibers, direct radar signal, or independent periodically synchronized clocks at all sites. However, the requirements are very high.

Analyzing various synchronization schemes requires knowledge on the used devices and different applications while the topic is somewhat confidential. More general analysis can be conducted using simulations to analyze only the effects of the synchronization errors on the detection probability or radar images. This way the results are not application specific but useful information on the relation between the errors and radar signals can be gathered. Eventually the results can be used to analyze if certain synchronization mean fulfills the set requirements.

This thesis introduces a MATLAB/Simulink simulation tool which can be used to model the interferences in synchronization signals and examine the effects. The tool imitates a general radar construction including illustrative blocks and modular structure allowing easy future modifications. Models of blocks are mainly ideal so far except the reference signal path. A survey for typical characteristics of blocks have been also made as a guideline for possible model modifications for more accurate practical components.

TIIVISTELMÄ

TAMPEREEN TEKNILLINEN YLIOPISTO
Sähkötekniikan koulutusohjelma
NIHTILÄ, TOMI: Monipaikkatutkan synkronoinnin simulointityökalu
Diplomityö, 74 sivua
Kesäkuu 2012
Pääaine: Elektroniikan laitesuunnittelu
Tarkastajat: Professori Karri Palovuori ja Professori Ari Visa
Avainsanat: tutkasimulointi, monipaikkatutkan synkronointi, pulssidopplertutka, tutkasignaalit

Tutka lähettää sähkömagneettisia aaltoja ja havainnoi ympäristöään kuuntelemalla heijastuvia kaikuja. Perinteisen monostaattisen tutkan lähetin ja vastaanotin sijaitsevat samassa laitteessa. Toteutus on yleisesti käytetty ja sillä on monia etuja. Sotilaskäytössä huomaamattomuus on kuitenkin toivottavaa ja eräs keino päästä siihen on erottaa tutkan lähetin ja sähkömagneettisesti näkymätön passiivinen vastaanotin toisistaan. Monipaikkatutkalla on lähetin ja useampia eri paikkoihin sijoitettuja passiivisia vastaanottimia. Tämä mahdollistaa myös kohteiden havainnoinnin useasta suunnasta, mikä auttaa havaitsemaan häivekohteita.

Eräs monipaikkatutkan toteutuksen haasteista on lähettimen ja vastaanottimen välinen synkronointi, jota tarvitaan vaihekoherenttiin toimintaan. Äärimmäinen vaihestabiilisuus tarvitaan pulssidopplerprosessointiin, joka on tehokkaan digitaalisen prosessoinnin perusta moderneissa tutkissa. Epästabiilisuus heikentää suorituskykyä, kuten havaitsemistodennäköisyyttä. Synkronointi voidaan toteuttaa erillisellä datalinkillä, optisella kuidulla, suoralla tutkasignaalilla tai erillisillä jaksollisesti tahdistetuilla kelloilla. Vaatimukset toteutukselle ovat erittäin tarkat.

Erilaisten synkronointitekniikoiden analysointi vaatii tietämystä käytetyistä laitteista ja eri sovelluksista, kun aihealue samalla on jossain määrin salassa pidettävä. Yleisempää tarkastelua voidaan kuitenkin tehdä analysoimalla simulaation avulla vain synkronoinnin virheiden vaikutusta havaitsemistodennäköisyyteen tai tutkakuviin. Tulokset eivät ole sovelluskohtaisia, vaan yleispätevä yhteys virheiden ja tulossignaalien välille voidaan johtaa. Tämän avulla voidaan myöhemmin analysoida täyttääkö tietty synkronointitekniikka asetetut vaatimukset.

Tämä työ esittelee MATLAB/Simulink-simulaatiotyökalun, jota voidaan käyttää mallintamaan häiriöitä referenssisignaaleissa ja tutkimaan vaikutuksia. Työkalu noudattaa geneeristä tutkan rakennetta ja on toteutettu havainnollisina lohkoina. Modulaarinen rakenne mahdollistaa helpon muokattavuuden jatkokehityksessä. Lohkojen mallit ovat toistaiseksi pääasiassa ideaalisia lukuunottamatta referenssisignaaleja. Lohkojen tyypillisistä virheistä on myös tehty yleisselvitys, jonka perusteella voidaan malleja lähteä tarkentamaan vastaamaan käytännön komponentteja.

PREFACE

I started working at the Department of Signal Processing in Tampere University of Technology in 2007 as a research assistant. A summer job prolonged and so did my studies. Everything ends eventually, luckily this time, since it is time to end my Master studies with this thesis.

This Master of Science thesis has been executed at the Department of Signal Processing in 2011-2012. The thesis is part of a research project funded by The Finnish Defense Forces and one part of the project has concerned radar systems, including multistatic radar.

Many people working for the project have been helpful when I have been working for this thesis. Thanks to Multimedia and Data Mining group for interesting coffee room talks, if not related to the thesis, often very interesting anyway! Special thanks in our group go to Juha Jylhä for being great help defining the topic and writing the thesis. Due to the nature of the thesis and definition of the topic many meetings have taken place where numerous people have helped defining the study, especially Timo Lensu and Antti Tuohimaa. Also thanks to Juuso Kaitalo, Jarkko Kylmälä, Seppo Horsmanheimo, and the examiners Karri Palovuori and Ari Visa.

Tampere, Finland
23 May 2012

Tomi Nihtilä
tomi.nihtila@gmail.com

CONTENTS

LIST OF ABBREVIATIONS

ADC	Analog-to-Digital Converter
AM	Amplitude Modulation
ARM	Anti-Radiation Missile
CPI	Coherent Processing Interval
CW	Continuous Wave
dBc	Decibels compared to carrier
dBd	Decibels compared to dipole radiator
dBFS	Decibels compared to full-scale output
dBi	Decibels compared to isotropic radiator
DFT	Discrete Fourier Transform
ENOB	Effective Number Of Bits
FFT	Fast Fourier Transform
FIR	Finite Impulse Response
FM	Frequency Modulation
FMCW	Frequency-Modulated Continuous Wave
GPS	Global Positioning System
HPRF	High Pulse Repetition Frequency
HRR	High-Range Resolution
I	In-phase
IF	Intermediate Frequency
IIR	Infinite Impulse Response
ISAR	Inverse Synthetic Aperture Radar
LNA	Low-Noise Amplifier
LO	Local Oscillator
LOS	Line of Sight
LPI	Low Propability of Intercept
LPRF	Low Pulse Repetition Frequency
LSB	Least Significant Bit
MPRF	Medium Pulse Repetition Frequency
MTI	Moving Target Indication
Q	Quadrature
PM	Phase Modulation
PRF	Pulse Repetition Frequency
PRI	Pulse Repetition Interval
RCS	Radar Cross Section
RF	Radio Frequency
RMS	Root-Mean-Squared (value)
SAR	Synthetic Aperture Radar
SFCW	Stepped-Frequency Continuous Wave
SINAD	Signal-to-Noise-and-Distortion Ratio
SNR	Signal-to-Noise Ratio
SNR+D	Signal-to-Noise-and-Distortion Ratio
WGN	White Gaussian Noise

LIST OF SYMBOLS

Chapter 2

E	Energy
P_r	Received power
P_t	Transmitted power
R	Range of a target
σ	Radar Cross Section (RCS) of a target
G_t	Antenna gain
A_r	Effective aperture area of an antenna
t_int	Integration time
f_c	Carrier frequency
τ	Pulse width
λ_c	Wavelength of carrier
c	Speed of light
f_PRF	Pulse repetition frequency
T	Length of signal period in time
t	Time
$a(t)$	Instant amplitude in a function of time
A	Peak amplitude
ω	Angular frequency, $\omega = 2\pi f$
ϕ_0	Initial phase
A_RMS	Root-Mean-Square (RMS) value
P_avg	Average power
R_ohm	Electrical resistance
D	Duty cycle
$A_\mathrm{RMS,sine}$	RMS value of continuous sine wave
$P_\mathrm{avg,sine}$	Average power of continuous sine wave
SNR	Signal-to-Noise Ratio
P_signal	Signal power
P_noise	Noise power
R_un	Unambiguous range
R_o	Range observed by the radar
ϕ_d	Phase difference
f_d	Doppler frequency
v_r	Radial velocity of a target
f_s	Sampling rate
δ_r	Range resolution
B	Bandwidth of the transmitted waveform
N_s	Number of frequency steps
Δf	Sampling interval in the frequency domain

t_{pmax}	Maximun round-trip propagation delay
θ	Azimuth angle
ϕ	Elevation angle
R_{t}	Bistatic range between transmitter and target
R_{r}	Bistatic range between target and receiver
L	Baseline; distance between transmitter and receiver
β	Bistatic angle

Chapter 3

f_{if}	Intermediate frequency
f_{lo}	Local oscillator frequency
f_{c}	Carrier frequency
$f_{\mathrm{c}} - f_{\mathrm{if}}$	Variable frequency
$a(t)$	Instant time-dependent amplitude
ω	Angular frequency, $\omega_0 = 2\pi f_0$
t	Time
ϕ	Phase angle
$\mathbf{A}(t)$	Rotating phasor with length A
j	Imaginary unit
f_{PRF}	Pulse repetition frequency
f_{out}	Output frequency components
n, m	Integers
f_1, f_2	Arbitrary frequencies
$s_{\mathrm{m}}(t)$	Information signal
$A_{\mathrm{m}}(t)$	Amplitude information
ϕ_{m}	Phase information
ω_{m}	Angular frequency of information signal
$s_{\mathrm{c}}(t)$	Carrier signal
ω_{c}	Angular frequency of carrier signal
$s_{\mathrm{AM}}(t)$	Amplitude modulated signal
μ	Modulation index
ω_{if}	Angular frequency of IF signal
ϕ_{if}	Phase angle of IF signal
λ_{c}	Wavelength of the transmitted RF signal
A_{d}	Range-dependent amplitude
$V(t)$	Instant time-dependent voltage
$\epsilon(t)$	Nominal frequency
$\phi(t)$	Phase noise
σ	Standard deviation
$\Delta f(t)$	Frequency fluctuation

Chapter 4

$r_{\mathrm{if}}(t)$	IF reference signal
f_{lo}	Local oscillator frequency
f_{if}	IF reference frequency
$r_{\mathrm{var}}(t)$	Variable reference signal
f_{c}	Carrier frequency
f_{var}	Variable reference frequency
$\phi_{\mathrm{s}}(t)$	Instant phase
$\phi_{\mathrm{FM}}(t)$	Phase generated by FM-block
μ_{FM}	FM modulation index
ω_{FM}	FM angular frequency
$\phi_{\mathrm{n}}(t)$	Phase noise
$p_{\mathrm{n}}(t)$	Signal consisting phase noise and FM
ω_{var}	Variable reference angular frequency
$a_{\mathrm{n}}(t)$	Amplitude noise (with mean 1)
$s(t)$	Output of *Interference and noise* block
f_{out}	Mixer output frequencies
n, m	Integers
f_1, f_2	Arbitrary frequencies
SNR_{ideal}	Ideal SNR of AD-converter
SNR_{j}	SNR limited by clock jitter
σ_{j}	Clock jitter RMS value
L_{dB}	MTI-attenuation in decibels
z_n	Complex pulse

1. INTRODUCTION

Originally the term radar was an acronym for RAdio Detection And Ranging. As the name implies, in its very basic form it uses radio waves to detect an object and determine its location. Different types of radars can be found for a variety of applications: airplanes, ships, weather forecasting, space technology, defense, security, and even conventional cars. Radar types differ a lot depending on the purpose. Whether the radar is designed for a moving or fixed platform, observing a car 10 meters away, or a missile 200 kilometers away obviously affects the type, size, power, and the operating parameters of the radar.

Technology related to radars has been a popular topic of research for a long time because of its crucial role as a main sensor in many applications. The importance of radar in military applications has been remarkable to hasten its technological development but it also has an essential function in aviation and weather forecasting. Vast amount of resources used for radar research has made it rather complex interdisciplinary device over time. Furthermore, the recent rapid development of technology, especially in the field of digital signal processing, has significantly improved the performance of radars but has also made them much more complicated. However, the principle of the operation remains the same.

Radar transmits electromagnetic waves via its antenna and observes its surroundings by listening to the echoes reflected from objects around. The strength of the reflections depends on the average transmitting power of the radar as well as a distance, size, shape, and materials of the object. The intensity of a propagating electromagnetic wave attenuates due to the spreading of the energy and the atmospheric attenuation. Furthermore, only a small part of the energy scatters back from the object to the direction of the measuring antenna. The same phenomenon occurs for all the obstacles and surfaces the propagating waves encounter generating infinite amount of signals summed together with different amplitude, phase, time and frequency characteristics. A challenging task of radar is to capture this signal and detect the possible objects of interest. Despite the often extremely weak interesting signal interfered with strong ground clutter, a term referring uninteresting reflections, and other electromagnetic interference, with the help of careful design and effective signal processing this task is possible.

Processing capabilities of radar are particularly important in the military field

since the task of the radar is to see as much as possible while not to be seen by hostile sensors. This leads to the restriction of radiated power while the receiver has to perform effective processing methods to be able to deal with the extremely weak signal returns. Another way to make a radar less visible is to use bistatic radar where the transmitter and receiver are located at the different sites, or multistatic radar where the setup has several receivers, and sometimes several transmitters as well, at different sites. [21, pp. 525-534]

1.1 Background of the Thesis

The advantages of multistatic radar are the electromagnetic invisibility of passive receivers and new perspectives for seeing targets. Passive receivers are more difficult to detect and destroy and thus can be located closer to the hostile ground in military applications. As they are also cheaper, several of them can be used to gain redundancy and to offer new perspectives which helps to detect stealth targets. They are designed to absorb some of the electromagnetic energy but mostly they just reflect the energy to other directions than the direction of arrival of the radar waves. This makes them difficult to detect with monostatic radar but multistatic radar has several receivers at different directions to detect the scattered energy. However, multistatic radars have some constraints and challenges in implementation and so far not many operational devices exist. [23, pp. 1-58] [21, pp. 525-534]

Oscillators and timing have crucial role in radar. Timing is needed for calculating signal propagation delays for range measurement. Accurate and very stable oscillators are needed for phase-coherent operation to effectively process the received weak signals. Digital circuits in modern radars also need stable clock signals. Unstable phase causes more noise and ineffective processing which eventually leads to decreased detection probability in surveillance radar or poor image quality in imaging radars. Timing circuits are drawn in simplified radar block diagram in Figure 1.1 where it can be seen that they are connected to all parts of the radar. However, in bistatic or multistatic configuration the parts are not located at the same site so the synchronization between the sites is needed. Modern rubidium and even quartz clocks are very accurate [23, pp. 258-259] and provide so stable time basis for applications that measuring the errors and instabilities requires special means [14, 15]. However, phase-coherent radar, especially in imaging applications, sets extremely high requirements for stability that no stand-alone clock system is enough without at least periodical synchronization between the transmitter and receiver [25, 4].

The original objective of the study was to analyze and compare synchronization means for multistatic radar. Synchronization can be implemented for example using the transmitted signal from the transmitter via land line, communication link, or direct signal propagation if line of sight exists between the transmitter and receiver.

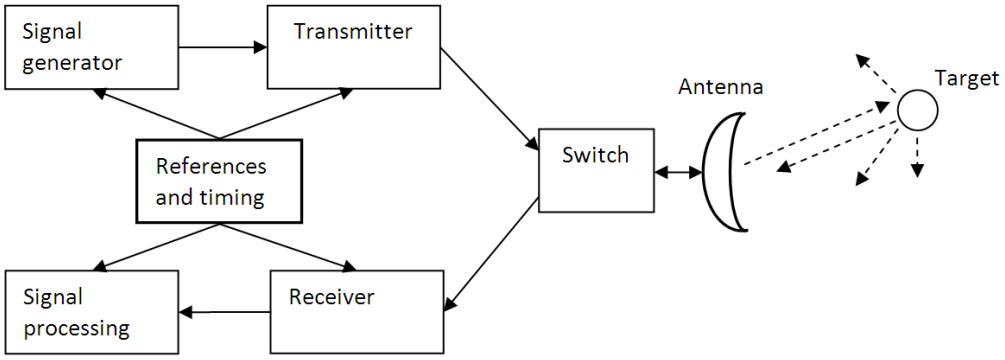

Figure 1.1: *Simplified radar block diagram.*

Periodically synchronized stable clocks on transmitter and receiver sites can be also used. One option for external synchronization signal is GPS [28] but at least in military applications it cannot be the only mean. [23, pp. 258-264], [28]

After literature survey and meeting with experts of the field it turned that comparison of synchronization means is a challenging task and requires lots of background work for comprehensive realization. Due to the lack of practical devices and the confidential nature of the potentially very effective operational systems not many documents and reports regarding to the systems exist, although, there are technical and scientific interest on multistatic radar and the amount of publications is growing. However, a decision was made to develop a tool for future analysis. With the tool, the errors and interferences in the synchronization and their effect on the radar signals, and with careful analysis the effect on the detection probability in a surveillance radar or the quality of the images in an imaging radar, can be examined. Thus, later when the specifications of the specific synchronization means of interest are known simulations can be made to analyze if the method fulfills the performance requirements.

1.2 Objectives of the Thesis

This thesis introduces an approach to simulate radar by modeling a radar transmitter and receiver and signals between them. Focus is on a multistatic setup where the transmitter and receivers are not located at the same site. Thus, the signal references and timing, or synchronization, between the transmitter and receivers need to be carefully considered. A simulation tool has been developed using MATLAB/Simulink software to analyze how noise and distortion in the transmission path of the synchronization signals affect the receiver performance and eventually, for example, detection probability. The simulation has been built from the beginning but a way to model high range-resolution radar in Simulink has been published in [6]. High range-resolution imaging radar is also an application of interest to model with

the simulation tool and to examine how interferences affect the quality of the images.

The simulation tool can model different types of errors in the synchronization path but many other parts are considered as ideal devices. However, due to the illustrative block diagram representation and modular structure of the simulation model it is rather easy to modify it to meet the desired level of modeling accuracy. The ideal models of components can be modified to imitate practical components with typical errors and nonlinearities, although, it needs time and knowledge to verify and validate these models. However, brief survey to some typical characteristics of radar components have been made. The simulated errors rely on the ones that can be verified using literature. If possible the results will be compared to the results of a real measurement radar.

The objective is to develop a simulation tool to model radar and at this point focus on the synchronization and reference signals of the radar, and also to understand the limitations and practical characteristics of components the simulation tool lacks. With this tool it is possible to model interferences and distortions and analyze their effect on the receiver performance, whether it is the detection probability of surveillance radar or image quality of an imaging radar. The simulations can be used for assessing and developing different radar concepts, especially when determining the cause-and-effect relationship of their low-level solutions to their high-level performance. The simulation tool can be also used to better understand the low-level operation of radar and examine what are the interference-sensitive parts. This way it can be possible to assess which are the components worth using resources to tweak the performance.

1.3 Structure of the Thesis

Chapter 2 introduces general radar theory and operating parameters emphasizing on a pulsed radar. Doppler processing and the concepts of bistatic and multistatic radar are presented. Chapter 3 continues radar theory inside the radar with a block diagram and describes the main components of radar. Some signal theory, models, and representations are introduced which are useful for the simulation. Finally oscillator and its possible interferences are explained as a basis for the simulation interference modeling. The theory in Chapter 3 is the basis for the implementation of the simulation tool.

Chapter 4 introduces the developed simulation tool block by block and ideas for future expansions of the used models. Chapter 5 presents the operation of the simulation tool by graphical illustrations and verifications of the implemented features as a results of the thesis.

Chapter 6 concludes the thesis by assessing the applicability of the simulation tool. Future development is considered and several prospects are suggested.

2. RADAR FUNDAMENTALS

Radar consists of an antenna, transmitter, and receiver, from which especially the latter two can be further divided into many smaller subsystems. In a conventional monostatic radar all these are located at the same site. This type of radar time-interleaves the use of the antenna for the transmitter and receiver; when the radar transmits it cannot receive and vice versa. In a bistatic configuration, the transmitter and receiver are spatially separated with their own antennas, setting new opportunities but also challenges. A multistatic radar is an expansion of the bistatic radar and contains several receiver antennas at different locations. [21, pp. 3-14]

Radars can also be divided into two main types based on the waveform: continuous wave (CW) and pulsed radars. A CW radar transmits the signal via its antenna continuously while listening to the echoes with another antenna. By sensing the Doppler shift caused by a moving target on the transmitted wave, the radar can determine the speed of the target. A conventional pulsed radar transmits a series of relatively narrow rectangular-like pulses and listens to the echoes between the pulses using the same antenna for transmission and reception. This type of radar can also sense Doppler shifts with some constraints. Pulsed operation not only prevents the high-power transmitter from interfering with the sensitive receiver but also allows straightforward range measurement. [21, pp. 3-14]

The fundamental feature of conventional pulsed radar is the ability to measure the range from the radar to a target by determining the propagation delay of a pulse traveling at a known speed, the speed of light. One of the basic features of radar is also a measurement of radial velocity, which is the component of the target velocity toward the radar, and it can be performed by sensing a Doppler shift or tracking the rate of change of range over a period of time. To determine the location of a target, along with its range also the angular direction of the target echo needs to be determined. This is done by using a scanning antenna with a narrow beamwidth to find the maxima of the target reflection. [21, pp. 3-14]

This thesis presents the properties and modeling of radar concentrating on a multistatic configuration. However, basic radar theory and signal models are applicable for all types of radar and are discussed in Chapters 2 and 3, respectively. The most essential references providing the background of the thesis are [21, 20, 11, 10, 8].

2.1 The Radar Equation

The strength of the echoes of the transmitted waves depends on the average transmitting power and a distance, size, shape and materials of the object, and losses also exist in different parts of the signal path. All these factors are put together in the radar equation, sometimes also called the range equation. It is not practical to calculate actual numerical values with it and it also lacks atmospheric attenuation and other losses, but it is useful for presenting dependencies between simple but important factors on the signal propagation path. By the radar equation, received signal energy

$$E = \frac{P_\mathrm{t} G_\mathrm{t}}{4\pi R^2} \frac{\sigma}{4\pi R^2} A_r t_\mathrm{int}. \tag{2.1}$$

It has been divided into four factors to represent the physical quantities. In the right side, the leftmost factor is the average power density at a distance R from the radar that radiates average power P_t via an antenna of gain G_t. The second factor represents the average power reflected back to the direction of the radar, σ being the RCS (Radar Cross Section) of the target, described below. The product of the first two factors is the power per unit area returned to the radar antenna having an effective area A_r. The first three factors multiplied equals to the average received echo power P_r by the antenna. Average power multiplied by integration time t_int results in the signal energy E, although, in practice integration is not perfect and some loss occurs. Signal power and energy are further discussed in Section 2.2 and integration in Section 2.4. However, it is worth noticing that the received energy is inversely proportional to the fourth power of the range when assuming RCS in question to be invariant regarding the range. Hence radar receiver must have very high dynamic range. [20, pp. 1.10-1.12], [21, pp. 135-149]

Whether the received energy is sufficient for a detection further depends on the noise level and on the processing capabilities of the receiver, briefly discussed in Section 2.4. Moreover, RCS of a typical target tends to fluctuate significantly over time due to changes in the aspect angle. RCS describes the effective area of the target and is a function of wavelength. However, only a sphere has a constant RCS at a certain wavelength while the RCS of a real target is a function of aspect angle and also depends on the material, shape and size (compared to wavelength) of the target. Real objects contain different materials and also the observed shape and size of the object varies depending on the angle of view. Some shapes tend to concentrate the reflections on the direction of arrival while others reflect the waves away which is preferred in stealth targets. Furthermore, an echo to a particular direction is a superposition of waves reflected from different parts of the object. Hence the RCS in a function of aspect angle may vary 20 dB or even 30 dB. This variation, observed typically from scan-to-scan, is called glint, scintillation, or fluctuation. RCS also

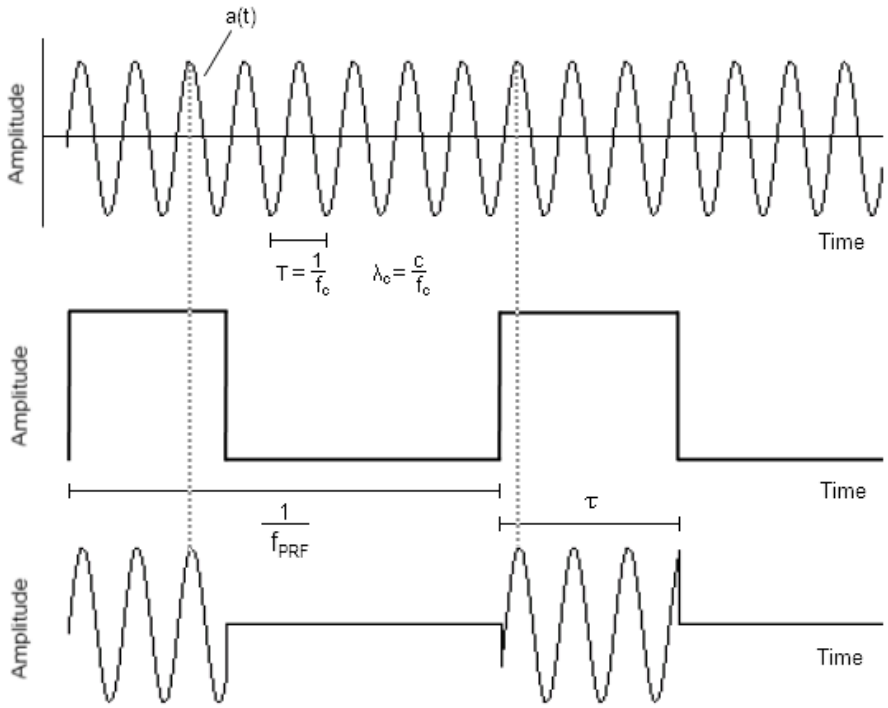

Figure 2.1: *Pulse train parameters in time domain. Dashed lines indicate the phase coherence of consecutive pulses compared to the continuous wave which usually holds true.*

has different characteristics for clutter, for example the RCS of volumetric clutter increases by second power of the range. More information and example figures of RCS can be read in [20, pp. 14.1-14.36].

2.2 Pulsed Waveform

Pulsed radar transmits pulse train with a certain pulse width, pulse repetition frequency (PRF), and peak power. Pulses are formed of a radio frequency (RF) carrier wave. PRF f_{PRF}, carrier frequency f_c, pulse width τ, and other signal notations described below are illustrated in time domain in Figure 2.1. Top wave is the continuous sine wave which is modulated by the square wave below it generating pulses of sine wave seen on the bottom waveform. Corresponding operation is performed in a radar transmitter. More signal parameters and representations are discussed in Chapter 3 but some signal nomenclature and parameters are introduced here. [21, pp. 107-114]

Signal Strength

Sine signal with a maximum amplitude of A, frequency f (Hz), angular frequency $\omega = 2\pi f$ (rad/s) and initial angle ϕ_0 can be represented as

$$a(t) = A \sin(\omega t + \phi_0), \tag{2.2}$$

where $a(t)$ is the instant amplitude or magnitude of the signal, varying in a function of time t and is limited between $-A$ and A. An electromagnetic wave propagates in space at a speed of light c (the speed in air is slightly slower but the difference is insignificant in this study). While period $T = 1/f$ is the length of one period in time, wavelength λ is the length in distance: $\lambda = c/f$. These parameters are shown in Figure 2.1 along with some other signal parameters. [26]

Another important parameter of a periodic signal, especially in electrical engineering, is the root-mean-square (RMS) value and it is defined as the name implies

$$A_{\mathrm{RMS}} = \sqrt{\frac{1}{T}\int_{t}^{t+T} a^2(t)\,\mathrm{d}t}. \tag{2.3}$$

Varying AC (Alternating Current) signal with RMS value of A_{RMS} volts produces the same power in a resistance as the constant DC (Direct Current) signal of A_{RMS} volts. Therefore, for DC signal the RMS value equals the (constant) amplitude of the signal, as can be noticed if $a(t)$ in Equation (2.3) is constant. Hence RMS value is related to the average power

$$P_{\mathrm{avg}} = \frac{A_{\mathrm{RMS}}^2}{R_{\mathrm{ohm}}} = \frac{\frac{1}{T}\int_{t}^{t+T} a^2(t)\,\mathrm{d}t}{R_{\mathrm{ohm}}}. \tag{2.4}$$

Solving Equations (2.3) and (2.4) for sine wave gives $A_{\mathrm{RMS,sine}} = A/\sqrt{2}$ and $P_{\mathrm{avg,sine}} = \frac{1}{2}A^2/R_{\mathrm{ohm}}$. In communications engineering R_{ohm} is often considered to be 1 ohm since it may be difficult to know the actual value and in signal comparisons it does not even matter. Hence it is often excluded in equations. When using the 1-ohm convention, amplitude squared can be considered as the instantaneous power $P_{\mathrm{inst}} = a^2(t)$. Integrating instantaneous power over time results in energy, and averaging it over time gives the average power, as is seen in Equation (2.3). [12, 5, 26]

The frequency of the pulse train, or the rate of pulses to be exact, in radar equals f_{PRF} (Figure 2.1) and average power can be defined using duty cycle $D = \tau/T = \tau f_{\mathrm{PRF}}$ and peak power. The power of the sine wave in Figure 2.1 is $P_{\mathrm{avg,sine}} = \frac{1}{2}A^2$ (when the resistance is excluded) and the average power of a pulse train of sine wave pulses seen on the bottom in Figure 2.1 is

$$P_{\mathrm{avg}} = DP_{\mathrm{avg,sine}} = \frac{1}{2}\tau f_{\mathrm{PRF}} A^2. \tag{2.5}$$

To be exact, an assumption has been made that pulse consists of an integer multiple of sine wave periods. The amount of full periods in one pulse is huge unlike in Figure 2.1 so this has no significance. The power in Equation (2.5) represents the power of electrical radar signal and like the radar equation (2.1) it shows the proportionalities

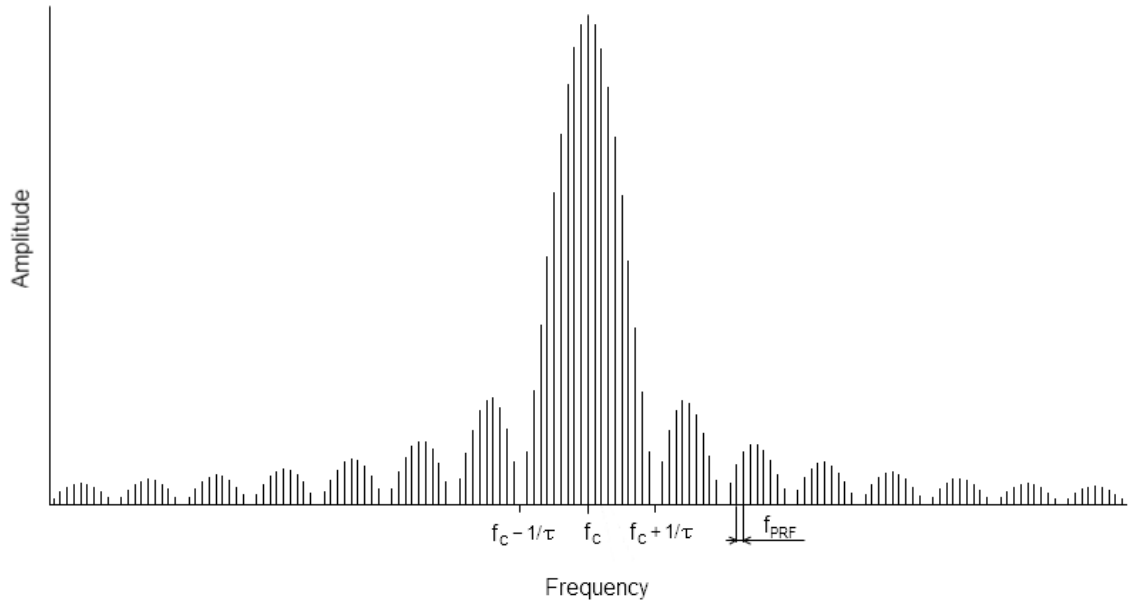

Figure 2.2: *Pulse train parameters.*

between factors. Furthermore, the transmitting power in the radar equation (2.1) can be replaced by the Equation (2.5) to further see the relationships between different parameters affecting the received energy. It should be also noticed, as will be seen in the following sections, that these parameters also affect other performance figures of radar and are also restricted by physical and practical constraints, hence they cannot be chosen only considering the power.

Signal energy always has to compete with the noise present in all real world systems. An important parameter for practical signals is the Signal-to-Noise Ratio (SNR)

$$SNR = 10 \log_{10} \frac{P_{\text{signal}}}{P_{\text{noise}}}, \tag{2.6}$$

comparing the signal power P_{signal} to noise power P_{noise} and expressed in decibels. The power of the signal returns may be on the order of noise so several pulses are usually integrated over time in Doppler processing introduced in Section 2.4. The effect of filtering on noise is presented in Section 3.5.

Frequency Spectrum

The Fourier transform of a rectangular pulse is a sinc function, and the narrower the pulse the wider the sinc in the frequency domain. The limit for this is the Dirac delta function having an impulse in the time domain and a constant value in the frequency domain. Figure 2.2 represents an example of the spectrum of a pulse train similar to the one in Figure 2.1 with some of its parameters. [7]

The shape of the spectrum is the same sinc function as with a single pulse, and

pulse width defines the width of the sinc main lobe as $2/\tau$ null-to-null bandwidth. Since pulses are not constant square wave but formed of the high frequency carrier, or the carrier wave modulated by the pulses, the main lobe peaks at the carrier frequency f_c instead of zero. Furthermore the spectrum is not continuous but series of spikes, which follows from the repetitive nature of the pulse train, forming the sinc envelope. The spikes are separated by the PRF. In fact they are not spikes but spread due to the finite length of the pulse train. This cannot be seen in Figure 2.2 but as Morris [11] states and shows the time domain parameters (in Figure 2.1) T, τ, $1/f_{\mathrm{PRF}}$ and the length of the pulse train have their corresponding frequency domain parameters f_c, $1/\tau$, f_{PRF} and the bandwidth of spectral lines, respectively. The spectral lines, which are not actually lines but Doppler spectra, are discussed in Section 2.3. [11, 2]

Pulse Repetition Frequency

Pulsed radar transmits a pulse and starts listening to the echoes where the time for the echo to return corresponds the distance it was reflected from. Radar cannot distinguish the pulses from each other without special means so the time period between the pulses must be long enough for the radar to receive the pulse before transmitting the next one. Range measurement is said to be unambiguous when pulse echo is received before the next pulse is transmitted so in that case the radar observes the true range of the target. Range is determined by measuring the propagation time of a pulse from a transmitter to a target and back, thus, the unambiguous range

$$R_{\mathrm{un}} = \frac{\mathrm{c}}{2f_{\mathrm{PRF}}} \tag{2.7}$$

where R_{un} is the unambiguous range. In case of a high-RCS target the echoes beyond the unambiguous range can be received. Then the next pulse is already transmitted and the radar interprets the echo as an echo of that pulse. Thus, the range observed by the radar in general is

$$R_{\mathrm{o}} = R \bmod R_{\mathrm{un}} = R \bmod \frac{\mathrm{c}}{2f_{\mathrm{PRF}}} \tag{2.8}$$

where R is the actual range of the target and R_{o} the range observed by the radar. However, this simplified case holds only for radars with unambiguous range measurement. Many radars use other means, such as pulse-to-pulse modulation sequences, to solve the range although echoes of several pulses are in the air at the same time. [21, 11]

Radars can be categorized by PRF in Low-PRF (LPRF), Medium-PRF (MPRF) and High-PRF (HPRF) radars. There are no specific numerical values to sepa-

rate the classes but the division is made by the ambiguity and hence depends on the supposed maximum range of the radar. An LPRF radar has the simplified unambiguous range measurement described above while an HPRF radar has an unambiguous Doppler measurement, discussed in Section 2.3. An MPRF radar uses other means for trying to solve both the ambiguous range and ambiguous Doppler measurements. An LPRF air surveillance radar may have a PRF of few hundreds hertz to give the unambiguous range of few hundreds kilometers, while an airborne fighter jet radar may have a PRF as high as 100–300 kHz. [21, pp. 325-334]

Carrier Frequency

Carrier frequency f_c is the frequency of the transmitted electromagnetic wave used for forming the pulses, as was seen in Figure 2.1. Carrier frequency may be constant or it can be varied in a function of time. Variation can be, for example, a linear frequency modulation within a pulse or frequency steps varying on a pulse to pulse basis. Modulation of the carrier frequency is typically done to make range resolution independent of the pulse length by increasing the bandwidth of it with the modulation. Range resolution and the effect of bandwidth on it is discussed in Section 2.5. [21]

Radar carrier frequency depends on the type of the radar and its application. Carrier frequency is related to the physical size of the radar antenna and the achieved directivity, discussed in Section 2.6, and the Doppler shift discussed in Section 2.3. The strength of the reflection from the target is also a function of wavelength because RCS is a function of wavelength. Moreover, some frequencies encounter more atmospheric attenuation and hence carrier frequencies are chosen from so called atmospheric windows where the attenuation is lower. As a result the choice of the operating frequency is made based on required performance but limited by physical constraints. Carrier frequencies are often divided into bands denoted by letters. There are different set of assigned letters and Table 2.1 presents one common set. Carrier frequency of a long range surveillance radar can be hundreds of megahertz while a missile seeker can operate near hundred gigahertz. [21]

Pulse Width

Pulse width, or length, τ is the duration of the pulse, typically with value from tens of nanoseconds to milliseconds depending on the type of the radar and the application. Pulse width along with PRF and peak transmitter power determines the average transmitting power (Equation (2.5)) strongly affecting detection range. Increasing PRF affects the unambiguous range and transmitting power cannot be raised without limits because of physical constraints and the military requirement for

Table 2.1: *Radar band letter designations, their frequency ranges, center frequencies and wavelengths of center frequencies [21, p. 85].*

Band	Frequency (GHz)	Wavelength (cm)
Ka	26.5-40	1.1-0.8
K	18-26.5	1.7-1.1
Ku	12.5-18	2.4-1.7
X	8-12.5	3.8-2.4
C	4-8	7.5-3.8
S	2-4	15-7.5
L	1-2	30-15

low probability of intercept (LPI) radar, which means a need for the radar to be as undetectable as possible. Hence a mean to increase transmitted power is to lengthen the pulse. However, as other parameters, lengthening pulse also has drawbacks. As will be presented in Section 2.5, the length of an unmodulated pulse is related to the range resolution of radar. Without some pulse compression method, increasing the duration of the pulse decreases the range resolution. Furthermore, monostatic radar cannot receive while transmitting so longer pulses cause longer times without reception widening the blind zones around the radar. [11]

2.3 Doppler Shift

Carrier signal is affected by Doppler shift when the radar and the target, which the echoes are reflected from, move with respect to each other so that the distance between them changes. In other words the range changes in a function of time. In case of a stationary pulsed radar receiving echoes from a moving target, the pulse is compressed or expanded in time depending on whether the target is moving towards the radar or away from it, respectively. Hence the carrier frequency increases or decreases due to the Doppler shift, the phenomenon illustrated in Figure 2.3. [21, pp. 189-198]

Doppler shift is used to discriminate moving targets from stationary objects such as ground clutter. Although clutter can be really strong and masking the signal return completely in the time domain, discrimination is possible in the frequency domain because of the Doppler shift. It can be done by a simple method called MTI (Moving Target Indication) or more sophisticated Doppler processing methods where the value of the Doppler shift can be measured. Since it is proportional to the range rate of the target, the velocity can be determined with certain constraints. With pulsed radars this is often referred to as pulse Doppler processing, see Section 2.4. [19]

It is worth noticing that in order to sense Doppler shift there has to be a change in range between the radar and the target in a function of time; the object must have a

(a) *Stationary wave source and moving object.*

(b) *Wavefronts compress due to approaching target.*

Figure 2.3: *Illustration of Doppler shift when moving target pushes wavefronts.*

velocity component on the line between the radar and the object. A target moving on a tangential trajectory with respect to the radar, for example, on a perfectly circular trajectory around the radar with a constant range, in theory would produce no Doppler shift. In such case the target may be invisible because of the much stronger ground clutter at the same zero hertz Doppler band, seen in Figures 2.4a-2.4c. [21]

Phase of Received Signal

The phase of the propagating electromagnetic wave is a function of time and position. The phase of the signal transmitted by the radar and reflected from the target depends on its initial phase and the propagation distance, or propagation time since the speed is known. When the target is at range R, the length of the propagation path is $2R$. This distance equals to $2R/\lambda_c$ carrier wave periods and multiplied by 2π gives the unwrapped phase. Since observed phase is $0...2\pi$, the theoretical phase of the received signal is

$$\phi_{\mathrm{d}} = -2\pi \left(\frac{2R}{\lambda_{\mathrm{c}}} \bmod \lambda_{\mathrm{c}} \right) \tag{2.9}$$

where the negative sign indicates a phase delay. In fact Equation (2.9) represents the phase difference due to the propagation which should be then combined with the initial phase. However, in practice radar receiver performs a phase comparison between the local reference, which represents transmitted wave, and the received wave and gets the phase difference. In pulse Doppler processing it is the rate of change of phase in consecutive pulses due to the change in range which matters rather than a single value of the phase. The phase presented here is interference-free ideal value. In practice all disturbances and noise in the propagation path and system also affect it. The purpose here is to show the formation of phase. The detection process including the signal phase detection is discussed in detail in

Section 3.2. An accurate modeling of the detection process is important owing to the application prospects of the radar model presented in this thesis.

Doppler Frequency and Spectrum

The phase expressed by Equation (2.9) varies in a function of time when the target range R varies in a function of time. Time derivative of phase is frequency so Doppler frequency f_d can be expressed by using the definition of frequency and Equation (2.9) and also assuming the target velocity is significantly slower than the speed of light:

$$f_\mathrm{d} = \frac{1}{2\pi}\left(\frac{d\phi_\mathrm{d}}{dt}\right) = -\frac{2}{\lambda_\mathrm{c}}\left(\frac{dR}{dt}\right) = -\frac{2v_\mathrm{r}}{\lambda_\mathrm{c}} \tag{2.10}$$

where v_r is the radial velocity, or range rate, of the target. Closing target has a positive Doppler frequency so the velocity of a closing target is negative. [11, 21]

Received pulses are sampled on reception to convert analog signals to digital samples. The sampling of the pulses is analogous to sampling of continuous wave when phase coherence requirement is fulfilled, which was illustrated in Figure 2.1 by the dashed lines. If one sample contains phase information presented by Equation (2.9), sampling the response of a stationary target leads to a constant phase with no difference between pulses and thus zero frequency. If the target is moving constantly respect to the radar the pulses sampled over time results in the frequency presented in Equation (2.10). However, Nyquist-Shannon sampling theorem [13] must be considered when when analyzing the phase difference between pulses or the generated Doppler frequency. When one sample per pulse is taken, the sampling frequency equals f_PRF and Nyquist frequency, which is the maximum frequency present in sampled system, is $f_\mathrm{PRF}/2$. This is the case with 1-channel receiver but usually 2-channel IQ-receiver is used. It takes two samples per pulse and doubles the effective sampling frequency, thus, it can resolve the sign of the Doppler frequency which tells if the target is approaching or receding. The frequency range is then $-f_\mathrm{PRF}/2...f_\mathrm{PRF}/2$. Detection, sampling, and IQ-reception are discussed in more detail in Chapter 3.

Aforementioned frequency range of f_PRF is the unambiguous Doppler frequency range, similarly as there was unambiguous range in PRF. The frequency components outside this range alias to this range and the observed Doppler frequency by the radar is

$$f_\mathrm{d} = \left(-\frac{2v_\mathrm{r}}{\lambda_\mathrm{c}}\right) \bmod f_\mathrm{PRF}. \tag{2.11}$$

As was mentioned in Section 2.2 and can be seen in Equation (2.11), carrier frequency affects the Doppler frequency. The unambiguous velocity range gets narrower when the carrier frequency increases but it also increases the sensitivity of the velocity

measurement since smaller change in velocity causes larger change in frequency. [21, pp. 189-198]

Low PRF causes strong aliasing of Doppler frequencies making velocity measurement heavily ambiguous because of the narrow Doppler spectrum. In Doppler or MTI processing the receiver distinguishes the moving target from the much stronger ground clutter by using Doppler shift. However, when the Doppler spectrum is aliased the ground return eclipses the spectrum at integer multiples of PRF forming so called blind speeds. Taking both Doppler spectrum aliasing and blind speeds into consideration PRF has a significant effect on the Doppler processing performance of the radar. However, the pulse repetition frequency is always a trade off between the unambiguous Doppler spectrum and the unambiguous range measurement and also affecting signal strength seen in Section 2.2.

Figure 2.4 illustrates four different Doppler spectra of IQ-receiver where the sign of the Doppler frequency can be resolved. All spectra include two targets from which one is a strong zero-Doppler echo representing ground clutter and the other a moving target with different speeds in different figures. The numerical values of PRF, speed, and carrier frequency are rather high and chosen for illustrative purposes. In Figures 2.4a—2.4c the weaker echo of the target can be easily distinguish from the ground reflections. However, in Figure 2.4d the generated Doppler shift is an integer multiple of PRF so the ground clutter eclipses the signal due to the aliasing of Doppler spectrum. In these figures it can be seen how Doppler frequency starts to repeat itself in the spectrum after reaching a value beyond the maximum unambiguous Doppler frequency of 125 kHz. Furthermore, the spectral lines which were seen in Figure 2.2 repeating themselves between f_{PRF} are actually the kind of spectra seen here in Figure 2.4. One way to interpret the target moving to the other side of the spectrum is to look at the larger scale picture and imagine it moving to the next copy of the Doppler spectrum (spike). Thus, the spectra of radar signals have several different scale phenomena inside them defining different characteristics. [11, pp. 48-62]

2.4 Pulse Doppler Processing

In order to get the Figures 2.4 seen above, some kind of processing needs to be done. The figures were generated using Fourier transform in MATLAB and radar receiver can perform similar signal analysis. IQ-receiver will be further explained in Chapter 3 but here it is assumed that all samples are complex $I+\mathrm{j}Q$ samples containing amplitude and phase information. The name and letters stand for In-phase and Quadrature-phase components since the complex component lags the real component 90 degrees. Radar must maintain phase-stable operation, shortly explained in Section 3.6, to be able to analyze consecutive pulses. Narrow Doppler

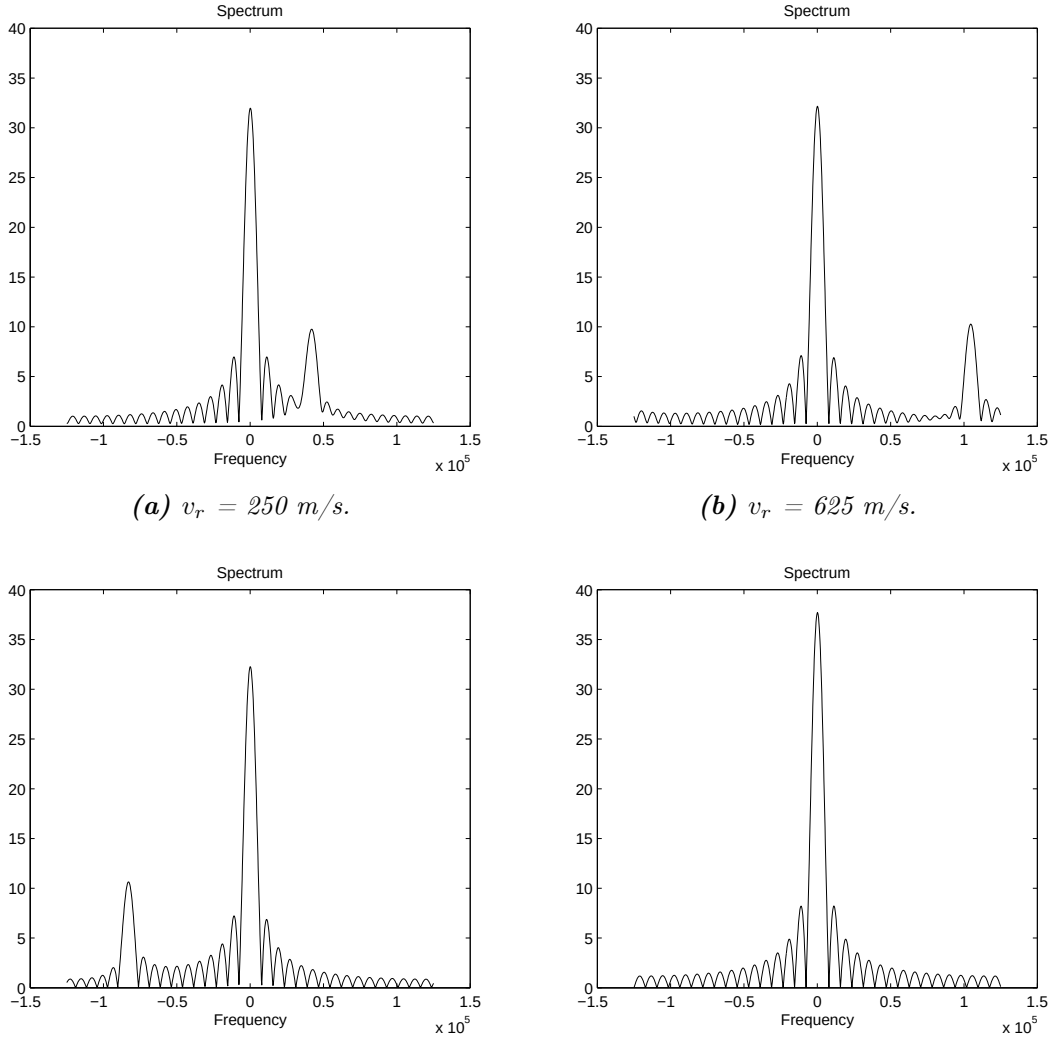

(a) *v_r = 250 m/s.* ***(b)*** *v_r = 625 m/s.*

(c) *v_r = 1000 m/s.* ***(d)*** *v_r = 1500 m/s.*

Figure 2.4: *Doppler spectra of ground clutter and a moving target with four different speeds. f_{PRF} = 250 kHz and f_c = 25 GHz.*

spectrum is lost in the pulse spectrum which can be realized by comparing Figure 2.2 and 2.4, and thus many consecutive pulses need to be analyzed to sense Doppler shift. [11, pp. 48-62]

The sequence of IQ-samples stored by the receiver can be arranged as a matrix illustrated in Figure 2.5. The numbers present the order of the received samples. Since pulse propagation time is proportional to the distance of an object, time can be converted to range. Thus a column in the matrix represents a time interval of one pulse repetition interval (PRI), the reciprocal of PRF. Each box in a column represents an IQ-sample stored at a sampling rate of the ADC, f_{s}. This dimension is referred as fast time and it represents the unambiguous range of the radar while each box represents an individual range bin, a certain area or volume around the radar. Range cell number 1 corresponds to the area next to the radar sampled immediately

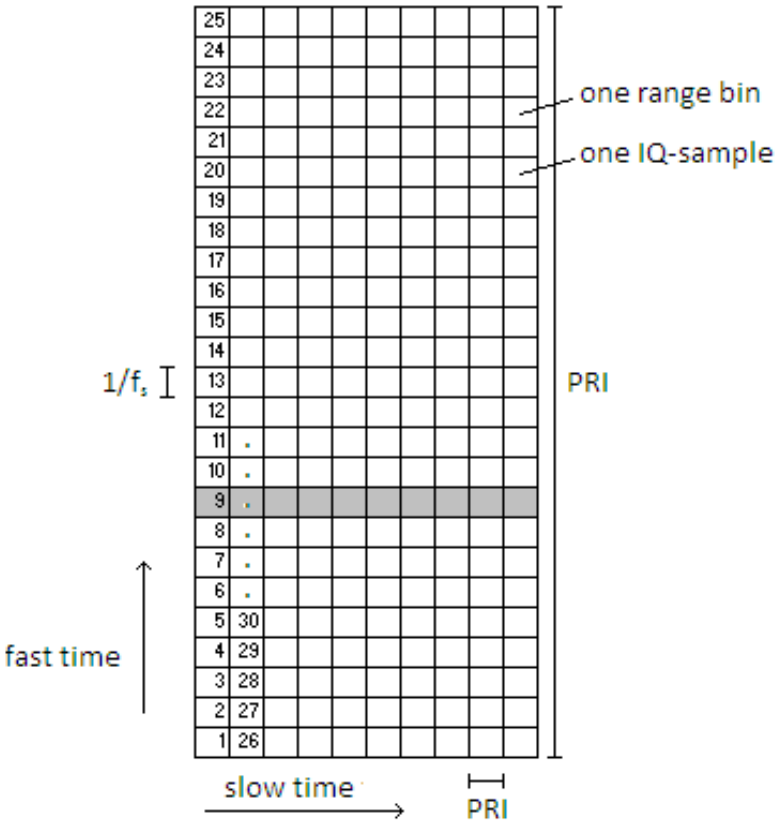

Figure 2.5: *Matrix of received samples. [11, p. 148]*

after pulse transmission while cell number 25 is the assumed maximum range, the unambiguous range. If echo is received beyond that, it will be interpreted as an echo of the next pulse coming from close range, from bin 26 on. [11, p. 148-149]

The area or volume one range bin corresponds depends on the radar and its parameters. Length is determined by the pulse bandwidth, explained in Section 2.5, while width is set by the antenna beamwidth, introduced in Section 2.6. Because of the spreading of a propagating pulse, width of a cell also widens with the increasing range. For the sake of clarity only 25 cells per PRI has been drawn, however, in reality the amount is significantly larger. [11, p. 148-149]

The horizontal dimension of the matrix in Figure 2.5 is considered as a slow time and has a sampling frequency of f_{PRF}. Spatially this represents the azimuth angle, explained in Section 2.6, while vertical dimension is the range. One row contains the data of one range bin in a function of time. In case of a conventional continuously scanning antenna, the range bin actually moves in a function of time. However, if the scanning rate is slow compared to the slow time, range bin can be considered to be static for a certain amount of time. Thus the processing to detect a target in a certain range bin is done for a row of samples, shaded in gray in Figure 2.5. [11, p. 148-149]

If radar receives ground echoes and echoes from a constantly moving target, performing Fourier transform for the row of samples results in something like Figures 2.4a—2.4d. Weaker signal peaks despite the stronger ground clutter if the Doppler frequency and radar parameters are suitable. Longer processing times, meaning more pulses, produces better frequency resolution and SNR. However, moving target may move to another range bin (another row in Figure 2.5) and the change in the state of movement, such as acceleration, weakens the result. Furthermore, the scanning antenna generates some modulation to the response. Typical coherent processing times (CPI), or dwell times, can be in the order of milliseconds. [21, pp. 135-149]

2.5 Bandwidth and Range Resolution

Range resolution describes the minimum distance of two objects that radar can distinguish from each other. With unmodulated pulse the range resolution is related to the length of the pulse:

$$\delta_r = \frac{c\tau}{2} = \frac{c}{2B}. \tag{2.12}$$

It is half of the spatial length of the pulse. The rightmost form is derived knowing that pulse bandwidth $B = 1/\tau$. Thus, range resolution can be also improved, meaning lowering the value of δ_r, by increasing the bandwidth of the pulse by other means than shortening it.

Shortening the pulse reduces the average power transmitted, hence, reducing the SNR and detection range so other means are necessary to increase the bandwidth. Pulse compression is a technique where long internally modulated pulse is transmitted and then compressed on reception by demodulating the pulse. The modulation can be frequency or phase modulation. Pulse compression is a broad topic to discuss here but more information can be found in [11, pp. 173-213] and [20, pp. 8.1-8.36]. Another mean of increasing the bandwidth is the stepped frequency waveform discussed below. It is easy to implement in demonstration purposes and simulations, as is presented in Chapter 4, but the disadvantage is the assumption for a target to be static for a rather long time.

Continuous wave is a simple example when examining the waveform bandwidth. If CW radar transmits constant frequency continuous wave, its bandwidth is zero and the range resolution equals infinity. Therefore such radar cannot measure the range without special means. If the wave is frequency modulated, usually linearly increasing or decreasing frequency in a function of time, it results in a frequency-modulated continuous-wave (FMCW) radar. Thus, the range can be determined as the difference of the transmitted and received frequencies compared to the sweep rate (Hz/s) of the modulation. A stationary target can easily be detected with

such a technique while a moving target or several targets require more complicated modulations. [21, pp. 177-186].

In a stepped-frequency continuous-wave (SFCW) radar a signal with a fixed carrier frequency is transmitted and received and then changed to another frequency until sufficient number of discrete frequency steps have been performed. The resulting data is a frequency response of the target with complex samples at N_s different frequencies. However, the measurement to hold true, the target needs to be stationary compared to the duration of the measurement. Measurement can be made faster by transmitting pulses of different frequency in a row but it causes challenges on the reception. [24]

After obtaining the frequency response of the target, it can be converted to a time domain representation by using the inverse Fourier transform. This results in a range profile with high range resolution since high bandwidth is used when measuring the frequency response corresponding to a short pulse in the time domain. However, since discrete frequency steps are used, Nyquist sampling criterion and the constraints set by it must be considered. The sampling interval in the frequency domain is the step size Δf. When using IQ-detection so that effective sampling rate is doubled compared to a one-channel receiver, a relation between the frequency step and the maximum propagation time can be obtained:

$$\frac{1}{\Delta f} = t_\mathrm{pmax}. \tag{2.13}$$

Therefore the frequency step determines the maximum unambiguous range

$$R_\mathrm{un} = ct_\mathrm{pmax} = \frac{\mathrm{c}}{2\Delta f}. \tag{2.14}$$

The unambiguous range corresponds the length of the range profile obtained using the inverse Fourier transform and is repeated every R_un. This is analogous to the repeatability of the Doppler spectrum with Fourier transform. The range profile is usually called down range. [24]

Figure 2.6 illustrates the range profile of two point scatterers 2 meters apart. A stepped-frequency waveform have been used with 32 frequency steps, a step size Δf being 5 MHz. From the Equation (2.12) it can be seen that the range resolution is $\delta_\mathrm{r} = c/2B \approx 0.9$ m. The two targets are easily separable. However, if unmodulated waveform was used, the range resolution would be $\delta_\mathrm{r} = c\tau/2 \approx 7.5$ m and the targets impossible to separate. Again the figure is similar to the Doppler spectra figures but now the x-axis is range instead of frequency because of the inverse operation.

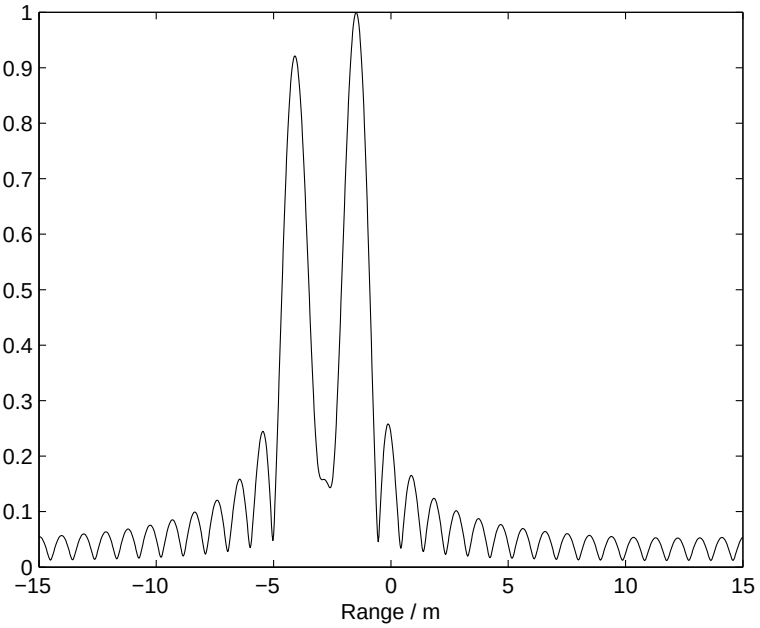

Figure 2.6: *Down range profile obtained by using stepped-frequency waveform with* $\Delta f = 5\ MHz$ *and* $N_\mathrm{s} = 32$. *Down range of 0 m implies the range in the middle of the measured range gate.*

2.6 Radar Antenna and Angular Resolution

Radar antenna is a device which directs the electromagnetic waves to propagate into space and gathers the weak echoes reflected from a target. Antenna type can differ but radar antenna is almost always a directive antenna focusing the radiated energy into a narrow beam. An antenna that produces a narrow beam has high gain and large effective area - certainly desirable characteristics for receiving weak echoes. Furthermore, the beamwidth also determines the angle resolution of the radar and with range resolution forms the spatial resolution. Discussing the antenna operation in great detail is beyond the scope of this thesis but more information can be found in [20, pp. 11.1-13.62] or books concentrated on antenna design and RF-electronics. However, some basic parameters are introduced here.

The most important antenna parameters are gain, radiation pattern, polarization, and bandwidth. Radiation pattern is a 2- or 3-dimensional plot representing the distribution of the radiated energy of the antenna. Angles in radiation patterns and descriptions of the orientation of the antenna are called azimuth and elevation angles, as is illustrated in Figure 2.7, and the central axis of the antenna is a boresight line. An example of a radiation pattern of a high-gain narrow-beamwidth directive pencil beam is presented in Figure 2.8. [21, pp. 91-106]

Gain is also connected to the radiation pattern since it is a measure of the directivity of the antenna. Antenna gain is a passive phenomenon - no power is added

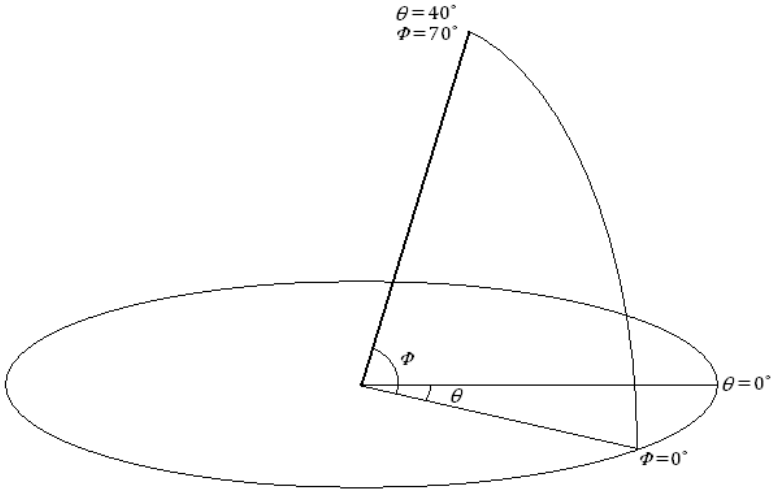

Figure 2.7: *Illustration of azimuth angle θ and elevation angle ϕ.*

to the system but the power is redistributed in a certain direction. When antenna directs the power distribution and creates a high gain mainlobe, sidelobes and backlobes also appear with nulls in between. These are unwanted since they waste power and can cause false detections and excessive reflections from the ground and nearby objects outside the boresight line. [21, pp. 91-106]

Another commonly used parameter, yet connected to the directivity and also to the angle resolution, is the beamwidth. It is expressed in degrees and is usually the width of the mainlobe between -3 dB points of its gain. The example in Figure 2.8 represents the radiation pattern of a high-gain narrow-beamwidth directive pencil beam. Usually three characteristics of radiation pattern are of interest: the width of the main lobe (the antenna beamwidth), the gain of the mainlobe (the antenna gain), and the relative gain of especially the strongest sidelobes (the decibel difference of the mainlobe and highest sidelobes). [21, pp. 91-106]

The gain G_t and the effective aperture area A_r, describing the size of the antenna relative to the wavelength and also related to the gain and directivity, can be expressed as

$$G_\mathrm{t} = \frac{4\pi A_\mathrm{r}}{\lambda_\mathrm{c}^2}. \tag{2.15}$$

Therefore, relatively large dimensions of the antenna compared to the wavelength results in a narrow beam and high directivity and gain. Gain is expressed with reference to a theoretical isotropic antenna, an antenna radiating equal amount of energy on all directions, thus having a radiation pattern of a sphere. The isotropic radiator has the gain of 0 dB while a dipole antenna has a gain of 1.76 dB. Sometimes the gain can be expressed relatively to the dipole radiator. Therefore the units dBi or dBd can be seen to distinguish if the reference is the isotropic or dipole radiator,

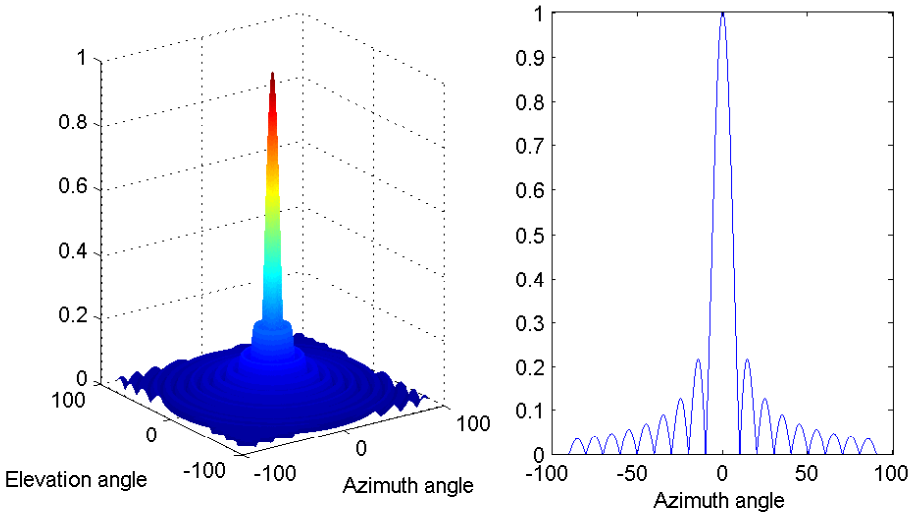

Figure 2.8: *Theoretical example radiation pattern and cross-section of a pencil beam at elevation angle of* 0°.

the difference being the aforementioned 1.76 dB. A high gain radar antenna may have a gain of 40 dBi. [21, pp. 91-106]

Antenna bandwidth defines the frequency response of the antenna. Many antennas operate in a relatively narrow frequency band, but the widening bandwidths set more requirements on that characteristic. As bandwidth and many other parameters or badly matched parameters can add attenuation to the signal path. Antennas can be linearly polarized with different angles or circularly polarized, or something in between. However, radars can also use cross-polarization where the transmitting and receiving polarizations are not the same. By this technique some more information about the target can be achieved, or it can be used to add more clutter attenuation, for example against rain. [20]

2.7 Bistatic and Multistatic Radar

Bistatic radar is a radar with separated transmitter and receiver sites. In a multistatic configuration there are many receivers, bistatic radar being a special case with one transmitter and one receiver. Target detection is similar to that of a conventional monostatic radar: transmitter illuminates the target while the receiver captures the echoes and processes the received signal. However, the scanning patterns of separate antennas need to be considered carefully. When determining a target location, a bistatic triangle, shown in Figure 2.9, must be solved. It contains the propagation time and angle measurements. When analysing a bistatic radar, similar equations can be derived than for a monostatic radar. However, detailed analysis is not presented here but a comprehensive analysis of the bistatic radar and its applications can be found in the Bistatic Radar book [23].

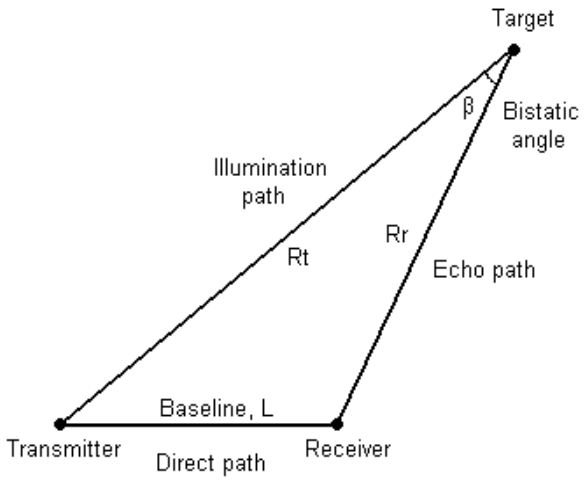

Figure 2.9: *Bistatic triangle with commonly used terms. [23]*

The advantage of the multistatic radar is that the receivers are invisible in an electromagnetic point of view, protecting them from anti-radiation missiles (ARM) and electronic jamming. Since they are not radiating anything, they cannot be easily seen by other radars or radiation locating equipment. Another aspect is that low-RCS stealth targets are often designed not to reflect the radar waves on the front direction. Most of the energy is still scattered to some directions and multistatic receivers may be able to capture these reflections. [8]

A fundamental problem of coherent multistatic radar is the synchronization between the transmitter and receivers to be able to perform all the processing described above. In monostatic radar the same stable local reference oscillator is used for transmitter and receiver for signal generation and detection, respectively. Two different synchronizations are needed for a multistatic radar: time synchronization for the range measurement and phase synchronization for the Doppler processing. Time synchronization can be accomplished using a communication link, a land line or a direct radio frequency signal if a line of sight exists between the transmitter and the receiver. Receiver can operate coherently if phase coherence can be established by synchronization of the local oscillators of the receivers. This can be achieved by similar means as with the time synchronization but the requirements are much higher. Stability requirements for monostatic radar are set by two-way pulse propagation time. The local reference which is used for phase comparison needs to be stable the time between pulse transmission and reception for the phase difference to be dependent only on the distance. For multistatic radar transferring the reference signal or using separate oscillators raises new considerations. Any disturbances on the way or instabilities weaken the phase accuracy of the reception. More about the synchronization issue can be found in Section 3.6. [23, pp. 258-265].

3. RADAR MODELING

Radar signal propagation path in its very basic form includes a signal generator, transmitter, antenna, propagation medium, target, receiver, and a processing unit, as was seen in Figure 1.1. Radar generates an electrical signal in its signal generator and shifts it to higher frequencies which can be radiated as electromagnetic waves via an antenna. The waves propagate in space and attenuate on the way due to spreading and encountering an atmospheric attenuation. Small amount of this energy hits a target of interest and scatters in space. Part of the scattered energy reflects back toward the radar receiver further spreading and attenuating. The radar antenna captures this energy, amplifies it, and processes it to obtain information about the target.

The radar receiver and the signal processing chain are vital when defining the end performance of the radar system because of the very low power of the captured radar signal. Furthermore, atmosphere is crowded with often much stronger undesired signal returns, commonly called as clutter, from ground, buildings, masts, and other objects of no interest. Electromagnetic interference of other devices than radar is also present everywhere. Thus, the receiver and processing stages have to distinguish the interesting signal from all the others.

The analog part of the receiver requires knowledge of RF-electronics and communications engineering while the digital processing part demands for skills on digital signal processing, digital electronics, and also communications engineering, not to mention the material science and mechanics in a real radar. Therefore large amount of theory is involved in radar technology and some suggestions for the literature to start with is [21, 20, 10, 11, 9].

This chapter mainly concentrates on the receiver side of the radar but most of the principles are also applicable in the transmitter side. The transmitter and receiver in a phase coherent radar are not operating as individual units but controlled by the common reference signals and timing circuits. These have to be also implemented in a multistatic radar when the transmitter and receiver are separated. Simulation tool presented in Chapter 4 allows the investigation of the sensitivity of these signals on the result. First a block diagram of radar is presented along with the propagation path of the radar signal. Before discussing radar signal reception and receiver components in more detail, means of modeling and representing signals are

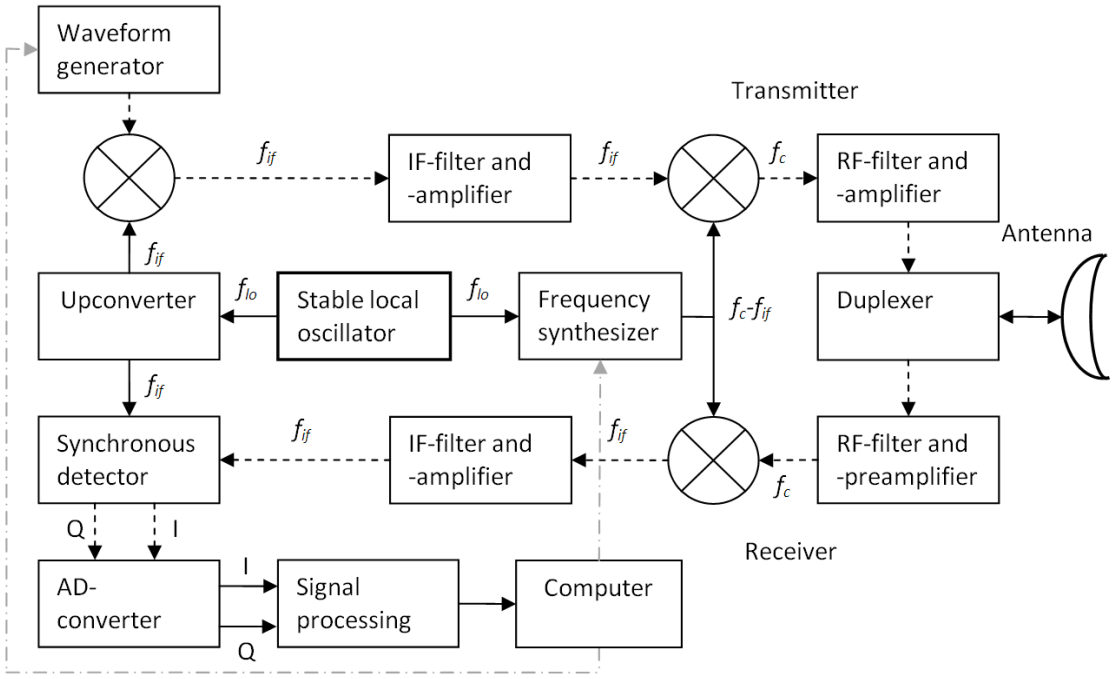

Figure 3.1: *Radar block diagram.*

presented. Signals are illustrated in time, frequency and phasor domains, which help expressing the signals present in radar. This Chapter is the basis for the simulation model introduced in Chapter 4.

3.1 Radar Block Diagram

More detailed propagation path of a radar signal inside the radar can be seen in a block diagram of the radar in Figure 3.1. Pulse train propagation is expressed with dashed lines while solid lines represent continuous reference signals. Mixer (a circle with a cross) stage produces the sum and difference frequencies of the frequencies fed to it, thus, allowing the shift of the signal to a higher or lower frequencies. Filters are then used to remove the unwanted components in the signal. Duplexer is a switch in front of an antenna and is needed when the same antenna is time-interleaved for transmission and reception. It alternately connects the antenna to a transmitter or a receiver and isolates the sensitive receiver from the high-power transmitter.

Mixer and frequency translation are discussed in more detail in Section 3.3 and detection in Section 3.4. Filters along with noise and how they interact are explained in Section 3.5. These topics are related to the simulation tool introduced in Chapter 4. There are other important components in radar as well but the details are beyond the scope of this thesis. Some practical aspects of components in modeling are discussed in Section 4.2.

Radar generates a baseband pulse train with a desired pulse length and PRF

in a waveform generator. The baseband signal is raised to radio frequencies, and it is done in several phases. The first mixer after waveform generator in Figure 3.1 raises the baseband pulses to an intermediate frequency (IF) f_{if}. IF-signal is then band-pass filtered and amplified. Filtering is needed to remove the unwanted components and to increase the SNR. The second mixer further moves the pulses up to the carrier frequency f_{c} ready to be transmitted via the antenna. Modulating a continuous wave signal with rectangular pulses in a mixer results in similar waveform as in the example of Figure 2.1 except one pulse can contain hundreds or thousands of sine wave periods.

For the sake of clarity only one IF stage is presented in Figure 3.1 but in practical radars there may be more to make frequency translation and filtering of image frequencies easier. Despite the number of stages, the principle of operation remains the same; the intermediate frequency stays constant while the frequency synthesizer output $f_{\text{c}} - f_{\text{if}}$ is changed if the carrier frequency f_{c} needs to be varied. This makes the design and implementation of the IF stage and IF-filters simpler.

On reception the captured RF signal is down-converted with a mixer from f_{c} to f_{if}. After filtering and amplifying the signal is detected in a synchronous detector discussed in more detail in Section 3.4. However, detector has two outputs: the In-phase (I) signal and the Quadrature-phase (Q) signal. Both the amplitude and phase information of the received signal can be extracted from these signals. These output signals are baseband signals corresponding to the waveform generator output on the transmitter side. The signals are low-pass filtered (anti-aliasing filter) and converted to digital signals for processing. A trend is to move the AD-converter closer to the antenna, for example, to the IF-stage when it is possible. This sets high requirements for the converter but the benefits of digital operation is achieved in the larger part of the receiver.

A low frequency stable local oscillator (LO) generates a continuous sine wave which is as immune as possible to the variations of environmental variables such as temperature, humidity, aging, and supply voltage. All the other frequencies in the radar are locked in and derived from the local oscillator. The upconverter creates a fixed IF and the frequency synthesizer generates the needed frequency ($f_{\text{c}} - f_{\text{if}}$) to create the desired carrier frequency (f_{c}). The simulation model presented in Chapter 4 follows this general block diagram introduced here.

3.2 Basic Signal Model

Before explaining the components of the block diagram in more detail, an illustrative way to represent radar signals is introduced. Continuous sine wave signal

$$a(t) = A\cos(\omega t + \phi) \tag{3.1}$$

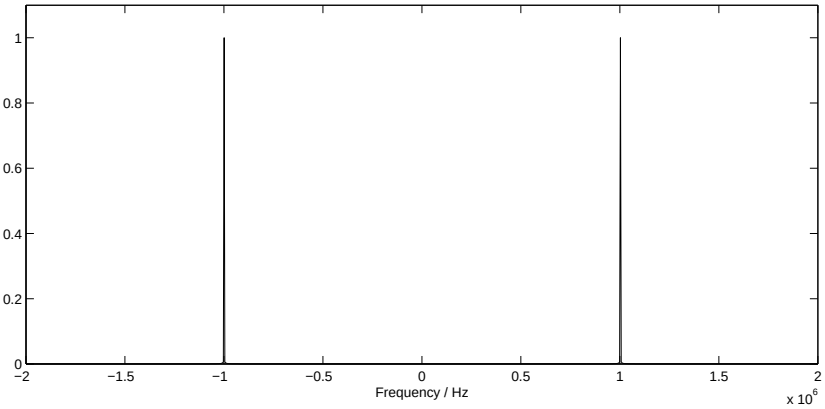

Figure 3.2: *Frequency domain representation of a sine wave with $f_0 = 1$ MHz.*

has frequency domain representation in Figure 3.2. Real sine signal has a reflected spectrum with respect to the zero frequency so the frequency components are f_0 and $-f_0$. One explanation for the negative frequency can be ratified in the phasor representation which is also used in literature [21, 10] to illustrate signals. The phasor representation of complex signal

$$\mathbf{A}(t) = Ae^{\mathrm{j}(\omega t+\phi)} \tag{3.2}$$

can be seen in Figure 3.3a. Phasor lies on the complex plane, has a length of A, rotates counterclockwise about the origin with an angular velocity of ω, and has an initial phase angle of ϕ. Phasor representations are used in [21] and [10] to illustratively present signals, noise, modulations, and Doppler shift.

The instant value of the Signal (3.2) can be considered as a frozen phasor but also a complex number or a vector on the complex plane. In general, when real or complex number is multiplied by $e^{\mathrm{j}\phi}$ the corresponding vector or phasor rotates counterclockwise on the complex plane by angle ϕ without affecting its length (absolute value). When a continuously increasing angle ωt is added, the phasor rotates.

Cosine signal is the projection of the rotating phasor on the real- or x-axis, seen in Figure 3.3a. By the trigonometric identities, cosine, or the real-axis projection, signal can be presented as

$$\cos(\omega t + \phi) = Re\left(e^{\mathrm{j}(\omega t+\phi)}\right) = \cos(\omega t + \phi) = \frac{1}{2}\left(e^{\mathrm{j}(\omega t+\phi)} + e^{\text{-j}(\omega t+\phi)}\right). \tag{3.3}$$

The sum of these two exponential functions, or rotating phasors, is always on the real axis. Thus real signal can be presented as two phasors rotating opposite directions, seen in Figure 3.3b. These phasors have opposite frequencies and in the spectrum of the real signal are two opposite frequency components. Similarly sine function can be represented by two exponential functions.

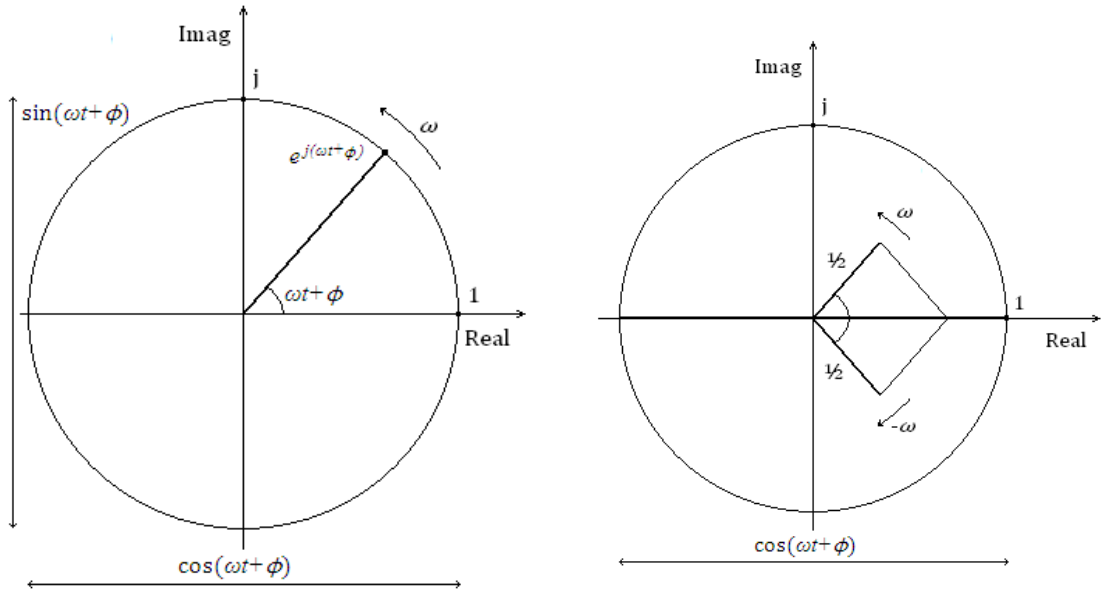

(a) *Complex signal has one rotating phasor. Projection of rotating phasor on the real and imaginary axes are the cosine and sine functions, respectively.*

(b) *Real cosine signal can be represented with two phasors rotating opposite directions resulting in the projection on the real axis.*

Figure 3.3: *Phasor representations of complex and real signals.*

Stimson [21] describes phasor diagram as a rotating phasor illuminated by a strobe light, hence resulting in a static figure when the strobe frequency equals the rotating frequency. If the reference, or the strobe light, stays constant while the signal encounters phase shift, the phasor starts to rotate in the following diagrams of frozen instants. The phenomenon has an analogy to the received radar signal and Doppler shift.

The signal reception of radar is a multi-stage system but the aforementioned situation can be considered between the synchronous detector and AD-converter in Figure 3.1. I- and Q-signals combined is a complex signal which can be represented as phasor. The receiver of pulsed radar takes a sample of the pulse and a phasor diagram can be considered as one complex IQ-sample. Sampling frequency equals f_{PRF} and corresponds the strobe light mentioned above. If target is stationary, consecutive phasor diagrams are the same. When the target moves, carrier wave encounters Doppler shift and phasor starts to rotate on the consecutive sampling instants.

Between two sampling instants, or pulses, phasor rotates a certain angle which over time forms certain frequency. The maximum frequency is achieved when the phasor rotates half revolution, or π, in a sampling period $1/f_{\mathrm{PRF}}$ s. This frequency is half of the sampling frequency, or the Nyquist frequency, $f_{\mathrm{PRF}}/2$. If the change of phase between samples is larger, the interpretation becomes ambiguous since it cannot be determined if the phasor actually rotated to that point from the other

direction, thus the absolute value getting smaller but the sign reversed. Similarly it cannot be known if the phasor rotates many full revolutions between the samples. If difference is 2π, the frequency is 0 Hz. This is one more interpretation for the sampling theorem and aliasing. The ambiguous frequency range is $-f_{\mathrm{PRF}}/2...f_{\mathrm{PRF}}/2$.

3.3 Mixer Frequency Translation

Frequency mixer is an important component in radars and other radio frequency devices. Mixer creates new frequencies from the frequencies fed to it and in radio transmitters and receivers it is used to shift signals from one center frequency to another. The important property of mixer is that the signal bandwidth and modulation remain intact in frequency shifting, or frequency translation. Frequency translation is needed since some operations can be only performed in low or high frequencies, or at constant frequency range. One such an operation is filtering where the ratio of the bandwidth and center frequency strongly affects the filter implementation. Changing the center frequency while the bandwidth stays intact allows varying this ratio. If this center frequency is kept constant by changing the frequency translation, the implementation of the filter is easier and the result better. This is also done in radar as was presented in the block diagram in Figure 3.1; IF is constant even if the transmitting frequency is varied. On the other hand, transmitted frequencies are determined by the type and requirements of the radar, the size of the antenna, government regulations, atmospheric attenuations, and other external reasons. By using frequency translation these does not have to affect the inner structure of the transmitter and receiver. Description of mixers in more detail can be found in [10, pp. 261-343].

If two signals with frequencies f_1 and f_2 are fed into a mixer which is a nonlinear device, the output frequencies are the harmonic and intermodulation components of these frequencies,

$$f_{out} = |nf_1 \pm mf_2|\,, \tag{3.4}$$

where n and m are integers $0, 1, 2, ...$ and $n + m$ the order of the response. The higher the order the smaller the output power, so the second order response is used in mixers so the desired output is $f_1 \pm f_2$. The unwanted components are filtered out, and the conversion scheme is designed so that none of the unwanted components are too close to the signals of interest. [10, pp. 264-265].

Since the sum and difference frequencies are used and other components filtered out, this can be used as an approximation of the mixer operation and is also used at this point in the simulation tool presented in Chapter 4. The generation of the sum and difference frequencies from two frequency components is the result of the multiplication of the signals in the time domain or the amplitude modulation. If

the information signal with amplitude information $A_\mathrm{m}(t)$ and phase or frequency information $\phi_\mathrm{m}(t)$

$$s_\mathrm{m}(t) = A_\mathrm{m}(t)\cos\left(\omega_\mathrm{m}t + \phi_\mathrm{m}(t)\right) \tag{3.5}$$

is multiplied with the carrier signal (with amplitude of 1)

$$s_\mathrm{c}(t) = \cos\left(\omega_\mathrm{c}t\right) \tag{3.6}$$

the result is

$$\begin{aligned} s_\mathrm{m}(t)s_\mathrm{c}(t) &= A_\mathrm{m}(t)\cos\left(\omega_\mathrm{m}t + \phi_\mathrm{m}(t)\right)\cos\left(\omega_\mathrm{c}t\right) \\ &= \frac{A_\mathrm{m}(t)}{2}\cos\left[(\omega_\mathrm{c}+\omega_\mathrm{m})t + \phi_\mathrm{m}(t)\right] + \frac{A_\mathrm{m}(t)}{2}\cos\left[(\omega_\mathrm{c}-\omega_\mathrm{m})t - \phi_\mathrm{m}(t)\right] \end{aligned} \tag{3.7}$$

using the known trigonometric identity $\cos(\alpha)\cos(\beta) = \frac{1}{2}\cos(\alpha+\beta) + \frac{1}{2}\cos(\alpha-\beta)$. Equation (3.7) shows that the level of generated components drops but also that possible amplitude and phase modulations pass the multiplication. [10, pp. 264-267]

The time domain multiplication of two signals is similar to amplitude modulation. If the amplitude of the carrier wave is modulated by the information signal,

$$\begin{aligned} s_\mathrm{AM}(t) &= \left[1 + s_\mathrm{m}(t)\right] s_\mathrm{c}(t) \\ &= \left[1 + A_\mathrm{m}(t)\cos\left(\omega_\mathrm{m}t + \phi_\mathrm{m}(t)\right)\right]\cos\left(\omega_\mathrm{c}t\right) \\ &= \cos\left(\omega_\mathrm{c}t\right) + \frac{A_\mathrm{m}}{2}\cos\left[(\omega_\mathrm{c}+\omega_\mathrm{m})t + \phi_\mathrm{m}(t)\right] + \frac{A_\mathrm{m}}{2}\cos\left[(\omega_\mathrm{c}-\omega_\mathrm{m})t - \phi_\mathrm{m}(t)\right]. \end{aligned} \tag{3.8}$$

Now also the carrier signal is present at the output which is true in many situations. The maximum amplitude A_m, or in general A_m divided by the carrier amplitude, is the modulation index μ which describes the depth of the modulation, usually in percents. [10, pp. 105-107]

Considering the receiver mixer 3 in Figure 3.1 the RF-signal captured by the antenna is filtered and amplified with a low-noise amplifier (LNA) and then fed to a mixer. This real signal of the frequency f_c can be expressed as

$$\cos(\omega_c t) = \frac{1}{2}\left(e^{j\omega_c t} + e^{-j\omega_c t}\right) \tag{3.9}$$

as was presented in Section 3.2. The second signal fed to the mixer is the frequency synthesizer signal of the frequency $f_\mathrm{c} - f_\mathrm{if}$:

$$\cos\left((\omega_\mathrm{c} - \omega_\mathrm{if})t\right) = \frac{1}{2}\left(e^{\mathrm{j}(\omega_c-\omega_\mathrm{if})t} + e^{-\mathrm{j}(\omega_c-\omega_\mathrm{if})t}\right). \tag{3.10}$$

Using the multiplication approximation for the mixer the output is

$$\begin{aligned}\cos(\omega_{\mathrm{ct}})\cos\left((\omega_{\mathrm{c}}-\omega_{\mathrm{if}})t\right) &= \frac{1}{2}\left(e^{\mathrm{j}\omega_{\mathrm{c}}t}+e^{\text{-}\mathrm{j}\omega_{\mathrm{ct}}}\right)\frac{1}{2}\left(e^{\mathrm{j}(\omega_{\mathrm{c}}-\omega_{\mathrm{if}})t}+e^{\text{-}\mathrm{j}(\omega_{\mathrm{c}}-\omega_{\mathrm{if}})t}\right) \\ &= \frac{1}{4}\left(e^{\mathrm{j}(2\omega_{\mathrm{c}}-\omega_{\mathrm{if}})t}+e^{\text{-}\mathrm{j}(2\omega_{\mathrm{c}}-\omega_{\mathrm{if}})t}+e^{\mathrm{j}\omega_{\mathrm{if}}t}+e^{\text{-}\mathrm{j}\omega_{\mathrm{if}}t}\right) \\ &= \frac{1}{2}\cos\left((2\omega_{c}-\omega_{\mathrm{if}})t\right)+\frac{1}{2}\cos(\omega_{\mathrm{if}}t).\end{aligned} \tag{3.11}$$

This sum signal is filtered with a band-pass filter, the bandwidth centered at IF, so that $2f_{\mathrm{c}} - f_{\mathrm{if}}$ component is filtered out. Similar analysis can be done on the transmitter side of the presented block diagram in Figure 3.1. However, when shifting the signal higher on the frequency band the lower component is filtered out.

3.4 Synchronous Detector

Detector shifts a signal from the IF further down and has an operation similar to a mixer. However, detector translates the signal all the way to the baseband ready for AD-converter to digitize it before processing. Detector signals can be examined the same way as mixer signals when performing a frequency translation from RF to IF as in Section 3.3. As is presented in Figure 3.1, the dashed line information signal from *IF-filter and -amplifier* block and the reference signal from *Upconverter* both have a frequency of f_{c}. As detector has a similar operation to mixer, also resulting in sum and difference frequencies, obviously the difference component is centered at zero hertz and is a baseband signal.

Similarly as with the mixer, now also including the phase of the signal, two signals are present: the information signal

$$\cos(\omega_{\mathrm{if}}t+\phi_{\mathrm{if}}) \tag{3.12}$$

is multiplied with the IF reference from the upconverter

$$\cos(\omega_{\mathrm{if}}t), \tag{3.13}$$

hence resulting in

$$\begin{aligned}\cos(\omega_{\mathrm{if}}t+\phi_{\mathrm{if}})\cos(\omega_{\mathrm{if}}t) &= \frac{1}{2}\left(e^{\mathrm{j}(\omega_{\mathrm{if}}t+\phi_{\mathrm{if}})}+e^{\text{-}\mathrm{j}(\omega_{\mathrm{if}}+\phi_{\mathrm{if}})}\right)\frac{1}{2}\left(e^{\mathrm{j}\omega_{\mathrm{if}}t}+e^{\text{-}\mathrm{j}\omega_{\mathrm{if}}t}\right) \\ &= \frac{1}{4}\left(e^{\mathrm{j}(2\omega_{\mathrm{if}}t+\phi_{\mathrm{if}})}+e^{\text{-}\mathrm{j}(2\omega_{\mathrm{if}}t+\phi_{\mathrm{if}})}+e^{\mathrm{j}\phi_{\mathrm{if}}}+e^{\text{-}\mathrm{j}\phi_{\mathrm{if}}}\right) \\ &= \frac{1}{2}\cos(2\omega_{\mathrm{if}}t+\phi_{\mathrm{if}})+\frac{1}{2}\cos\phi_{\mathrm{if}}.\end{aligned} \tag{3.14}$$

After low-pass filtering only the constant phase-dependent component remains. In

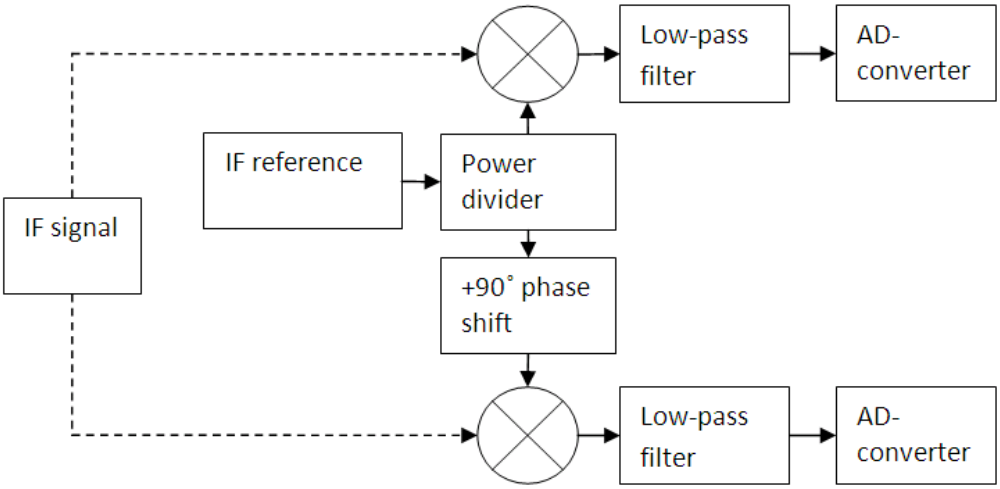

Figure 3.4: *Synchronous detector block diagram. IF signal is the input to synchronous detector in Figure 3.1.*

general, as was discussed in Section 2.3 and presented with Equation (2.9), the phase difference between the transmitted and the received wave depends on the range of the target. When the result of Equation (3.14) is combined with Equation (2.9), the signal magnitude after detector, also considering low-pass filter and merging amplitude $\frac{1}{2}$ to the A, is

$$A_{\mathrm{d}} = \cos\left(-2\pi\frac{2R}{\lambda_{\mathrm{c}}}\right). \tag{3.15}$$

As the wavelength λ_{c} is fixed, the magnitude of the received signal after the detector depends on the range of the target. Thus, even a constant-RCS moving target generates a varying magnitude signal, the phenomenon not to be confused with RCS fluctuation or scintillation. Furthermore, targets can lie in blind spots where the amplitude goes to zero.

To prevent the magnitude variation due to range, and to make Doppler processing possible, modern radar with a synchronous detector, also called IQ-demodulator or coherent detector, uses I and Q channels to detect the signal phase and amplitude. It performs a frequency conversion and generates a complex signal I+jQ centered at zero frequency. To achieve that a phase delayed version of the IF reference is used together with the original reference. An illustration of a synchronous detector is presented in Figure 3.4. [20]

The IF reference is split into two signals with the phase difference of 90°, or $\pi/2$. The convention is to have the Q lagging the I by 90°. Depending on the configuration different signs for the phase difference of the IF references need to be used to achieve the desired output where Q lags I. Hence in the example here the second reference

leads by 90°. The leading reference

$$\cos\left(\omega_{\mathrm{if}}t + \frac{\pi}{2}\right) = -\sin(\omega_{\mathrm{if}}t) \tag{3.16}$$

is multiplied with the Signal (3.12):

$$\begin{aligned}\cos(\omega_{\mathrm{if}}t + \phi_{\mathrm{if}})\left(-\sin(\omega_{\mathrm{if}}t)\right) &= \frac{1}{2}\left(e^{\mathrm{j}(\omega_{\mathrm{if}}t+\phi_{\mathrm{if}})} + e^{-\mathrm{j}(\omega_{\mathrm{if}}+\phi_{\mathrm{if}})}\right)\frac{1}{\mathrm{j}2}\left(-e^{\mathrm{j}\omega_{\mathrm{if}}t} + e^{-\mathrm{j}\omega_{\mathrm{if}}t}\right) \\ &= \frac{1}{\mathrm{j}4}\left(-e^{\mathrm{j}(2\omega_{\mathrm{if}}t+\phi_{\mathrm{if}})} + e^{-\mathrm{j}(2\omega_{\mathrm{if}}t+\phi_{\mathrm{if}})} + e^{\mathrm{j}\phi_{\mathrm{if}}} - e^{-\mathrm{j}\phi_{\mathrm{if}}}\right) \\ &= -\frac{1}{2}\sin(2\omega_{\mathrm{if}}t + \phi_{\mathrm{if}}) + \frac{1}{2}\sin\phi_{\mathrm{if}}\end{aligned} \tag{3.17}$$

which is the Q signal and the result of Equation (3.14) is the I signal. These are low-pass filtered, amplified by two, and combined to get the synchronous detector output

$$I + \mathrm{j}Q = \cos\phi_{\mathrm{if}} + \mathrm{j}\sin\phi_{\mathrm{if}} = e^{\mathrm{j}\phi_{\mathrm{if}}} \tag{3.18}$$

which is the complex phasor discussed in Section 3.2. This signal is also a function of the phase ϕ_{if} and thus a function of the range of the target. However, the range does not affect the amplitude of the signal but the phase of it which is the needed result for the Doppler processing. The result given here is a counter-clockwise rotating phasor when the target is approaching resulting in a positive Doppler frequency which is a convention in radar theory. Depending on the frequency conversion schemes, the sign of the phase difference of the IF-reference, or the sign of the I or Q sample in the processing stage, may need to be changed to achieve the mentioned convention. Here the sign of the IF-reference was changed. [20, pp. 6.31-6.35]

After discussing about the IQ-detected and range-independent amplitude it should be noticed that in practice the amplitude scintillates because of the changing RCS which is a significant phenomenon with practical targets. However, by preserving the phase information the radar can perform an efficient integration of several pulses over a certain period of time by Doppler processing as was described in Section 2.4.

3.5 Noise Filters

Filters are used to pass wanted signals or remove unwanted signals, or in general to change the amplitude and phase of certain frequencies. Filters can be analog or digital both having their own advantages and disadvantages as well as limitations. Filters at the highest frequencies are analog since these signals cannot be converted to digital. Digital filters are commonly used where it is possible because they often offer better performance and do not significantly suffer from varying environmental variables such as temperature, humidity, aging and mechanical disturbances. Dig-

ital filters can be also steeper and more selective than their analog counterparts. Some filter theory and analog filters are discussed in [10, pp. 143-260] and in many electronics books, and digital filters as well as comprehensive filtering theory in the time and frequency domains in [3].

Filters are used in radar between different parts to remove unwanted signals such the image frequencies and unwanted mixer output components. Filters from RF until anti-aliasing filter of the AD-converter are analog and after that digital. Besides removing unwanted signals, another task of filter is to remove noise outside the bandwidth of the signal of interest. Filters are considered here from this point of view and noise introduced since it is an important part of the simulation tool presented in Chapter 4. Other filter characteristics can be found on the books mentioned above.

Noise can be characterized by its frequency and amplitude distributions. The most common type of noise is the white Gaussian noise (WGN) referring to the flat frequency spectrum and Gaussian-shaped amplitude distribution usually with zero mean value. Other frequency distributions, or colors, are $1/f$ noise which is often called pink or flicker noise and $1/f^2$ noise called red or brownian noise. The spectrum can also be more complex as often is the phase noise in oscillators. An example of a different amplitude distribution is the quantization noise of an analog-to-digital converter which has a uniform distribution.

Noise need to be examined in a limited bandwidth because otherwise the power would be infinite due to the infinite frequency spectrum. Since white noise has a constant power spectrum, the power is directly proportional to the bandwidth. Thus white noise is a theoretical concept and in practice it is always bandwidth-limited, nevertheless called white noise. In practice the bandwidth is always limited by some physical constraints. Two examples of sine signals with additive white Gaussian noise with different noise bandwidths are presented in Figure 3.5. The noise power spectral density (Watts / Hz) is the same in both signals. The signal in Figures 3.5a and 3.5b has a noise bandwidth of 500 MHz and SNR of 7 dB. By limiting the bandwidth to one tenth, 50 MHz, the SNR is raised 10 dB to 17 dB, seen in Figure 3.5c and 3.5d. Despite the equal noise power density the former one has higher overall noise power due to the larger bandwidth.

In analog systems the noise bandwidth is infinite in theory and in practice limited by parasitic impedances. However, in digital systems the sampling frequency limits the noise bandwidth to some known and reasonable value since no frequencies higher than the Nyquist's frequency can exist in the signal. The signal can be further filtered inside the system to further limit the bandwidth. In the example above the sine wave stays intact when lowering the bandwidth. Therefore, the signal power remains constant and SNR is improved by the factor the noise power is reduced.

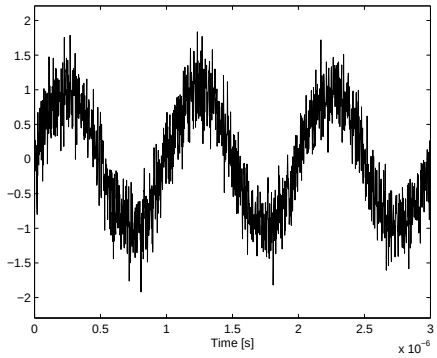

(a) *Time domain, 500 MHz BW, SNR = 7 dB.*

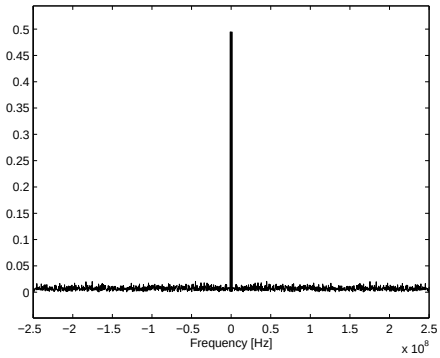

(b) *Frequency domain, 500 MHz BW, SNR = 7 dB.*

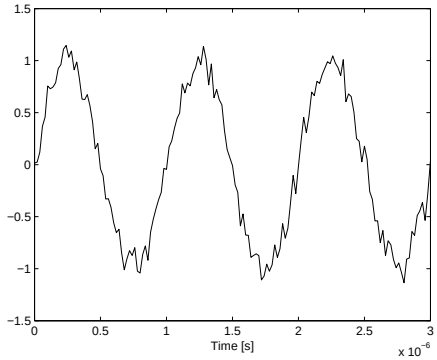

(c) *Time domain, 50 MHz BW, SNR = 17 dB.*

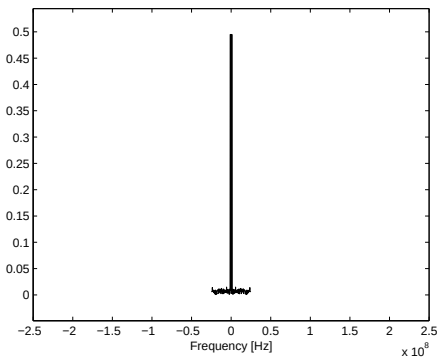

(d) *Frequency domain, 50 MHz BW, SNR = 17 dB.*

Figure 3.5: *1 MHz sine wave with two different noise bandwidths. In spectra the two signal spectrum spikes are close to each other and appear as one thick spike. In Figures a-b noise bandwidth is 500 MHz resulting in SNR of 7 dB with the added noise spectral density. In Figures c and d the bandwidth has been reduced to 50 MHz resulting in SNR of 17 dB.*

When more complex signal is used, at some point some signal power starts to filter out as well. The optimal filter to maximize SNR is called a matched filter and it is generally used in communications engineering. Mathematically the impulse response of the ideal matched filter is the time-reversed complex-conjugate of the signal to be filtered.

3.6 Oscillator

Oscillator and timing circuits play crucial role in radar. Typically first local oscillator needs to be stable low frequency oscillator, which is as immune as possible to the variations of environmental variables, is used and other oscillator and timing circuits, and frequency synthesizers are locked in and derived from this oscillator. Stable phase-coherent operation is needed for the Doppler sensing and processing and accurate timing for range measurement. Stable digital clock signals are needed

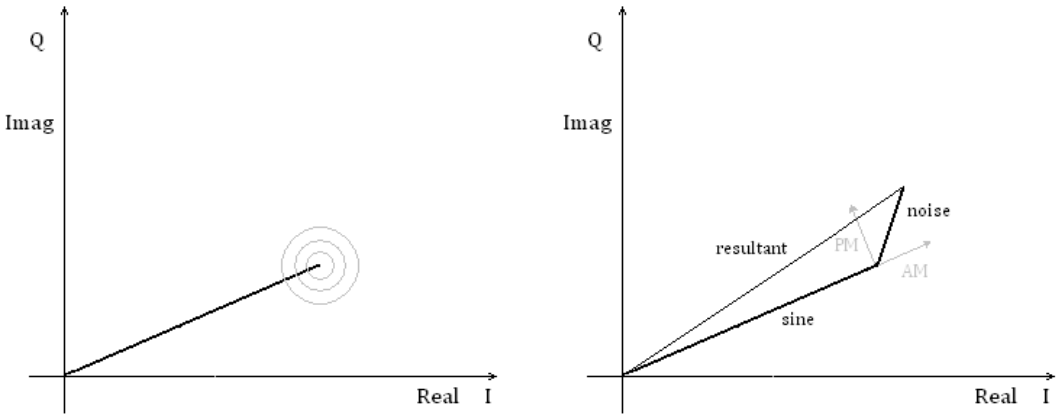

(a) *Noise is a statistical phenomenon so its RMS value can be presented in circles of propabilities.*

(b) *Noise can be split into amplitude (AM) and phase (PM) components.*

Figure 3.6: *Noisy reference sine signal is the sum of the ideal signal and noise.*

for processing and especially AD-converter. [20, pp. 6.14-6.18]

In theory oscillator output would be pure sine wave but in reality it contains interferences and instabilities which can be characterized both in the time and frequency domains. A model for oscillator signal can be generated similarly than in earlier sections. Oscillator output voltage

$$V(t) = [V_0 + \epsilon(t)] \sin [2\pi f_0 + \phi(t)] \tag{3.19}$$

where V_0 and f_0 are the nominal amplitude and frequency, respectively, and $\epsilon(t)$ is the amplitude noise, and $\phi(t)$ the phase noise. These noise components in phasor signal are shown in Figure 3.6 where AM (Amplitude Modulation) represents $\epsilon(t)$ and PM (Phase Modulation) $\phi(t)$. This separation of noise into components is rather theoretical but they can have different frequency characteristics. In high-performance sources amplitude noise, or $\epsilon(t)$ in Equation (3.19), is usually negligible and phase noise is of interest. It can be also noticed that these components affect unequally the signal when considering the real signal as the projection on the real axis. For example, in zero crossings AM has no effect but PM causes uncertainty to the zero crossing instant. In digital clock signals this is often called clock jitter, and for example in AD-converter it causes noise and distortion because of the variation of sampling instances. Figure 3.6a shows the circles of noise values where they can represent for example σ, 2σ, and 3σ values if the statistics are Gaussian. If the real and imaginary components of the noise are independent and Gaussian distributed, the length of the noise phasor, or the magnitude, is Rayleigh distributed and the phase angle uniformly distributed [10, pp. 102-103]. [17], [10, pp. 345-360]

Oscillator interferences have effect on the radar performance. It is assumed that

the propagation path of synchronization signal can cause or increase similar effects as in oscillators introduced here and in [10, pp. 345-360], [17], and [20, pp. 6.14-6.18]. Thus, the noise separated into AM and PM components as well as amplitude and frequency modulations for slower effects are modeled in the simulation tool as reference signal errors.

Bistatic and multistatic radars need two different synchronizations: time and phase synchronization. Time synchronization is needed to adjust the timing of the reception for range measurement. Timing accuracy is typically on the order of a fraction of the pulse length. The synchronization can be implemented for example using the transmitted signal from the transmitter via land line, communication link or direct signal propagation if line of sight exists between transmitter and receiver. Periodically synchronized stable clocks on transmitter and receiver sites can be also used. If direct propagation path or external link is used, the propagation errors dominate and need to be carefully considered. Phase synchronization between transmitter reference and receiver reference with much higher requirements is needed for phase-coherent operation for Doppler processing. Synchronization can be implemented by locking the receiver to the transmitter or by periodically updating accurate clocks. However, the accuracy requirements are higher than in time synchronization and depend on the needed phase accuracy. This can be from less than one degree to tens of degrees of phase meaning many decades higher accuracy than in time synchronization. One major difference between monostatic and multistatic radar is that low-frequency effects cancel out in monostatic radar because the variations are insignificant during the pulse propagation time while in bistatic or multistatic radar these errors may be additive instead [28]. Also in the simulation time-consuming imaging methods wanted to be used and therefore the possible coherent time for the reference is much longer. [23, pp. 258-259]

4. SIMULATION ENVIRONMENT

A simulation tool has been developed to allow examining the operation of radar. The structure of the simulation model follows the general construction of pulsed Doppler radar which was discussed in Chapter 3 and illustrated in Figure 3.1. However, focus has been in the simulation of multistatic radar so modeling the timing and phase coherence has been the main aspects in developing the simulation model. Since the simulation tool has a modular structure, it is easy to adjust the model to meet various needs or to enhance the model by adding more features into it and making it more accurate. The tool has been created using MATLAB/Simulink software. The system consists of the signal generation, transmission, reception, reference transmission, and the target model, and it is created by using generic Simulink blocks and embedded MATLAB code. Initializations and the processing of the output data are executed with conventional MATLAB scripts and functions and graphical user interface is under development. Despite the reference interferences which are the main aspect of the model, ideal models of components have been used. Some ideas to modify the ideal models to represent practical components better are presented in Section 4.2

Radar configuration in simulation is bistatic radar with transferred reference signals which can model fiber optics or other direct transmission of references. This setup was chosen because of specific interest in one real experimental radar. Waveform options are versatile and carrier frequency, PRF, and pulse width can be chosen, and also the carrier can be varied in sequences. The stepped-frequency waveform can be used to achieve high range resolution. The group of pulses running throughout the bandwidth of the waveform from the lowest to the highest frequency is called burst. Similarly as PRF there is a burst rate which is much lower than the PRF, for example in case of 128 pulses 128 times lower. One of the purpose of the simulation is to offer a possibility to experiment what are the stability requirements for the reference signals in the burst repetition interval which can be significantly longer than pulse repetition interval, and how the end signal is affected if the reference is not within the accuracy limits. Thus, as the point of the simulation is to model references with interferences it is made easily possible.

Simulink simulation is executed by calculating the system variables and states at discrete time steps, simulation steps, which are the fundamental time units of the simulation. That also represents the fundamental sampling frequency of the

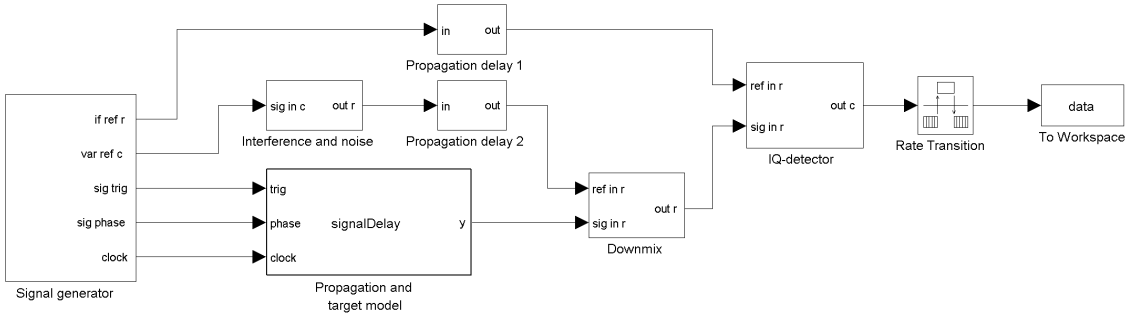

Figure 4.1: *Top level block diagram.*

system limiting the frequencies that can be expressed without aliasing, considering Nyquist-Shannon sampling theorem [18, 13]. Simulink offers a possibility to model continuous time system by internally simulating continuous time system by dividing simulation steps into smaller substeps and solving the state of the system more frequently. Simulation step can be chosen to be fixed or variable, the latter varying based on the derivatives of the signals in simulation. However, to have the most controlled awareness of the operation of the simulation, discrete time operation and fixed simulation step have been chosen. The changes on the initialization of the simulation are done in matlab script.

4.1 Introduction of Simulation Tool

The top level block diagram of the simulator is in Figure 4.1 and block functions are explained in more detail in the following sections. Important signals in top level block diagram are shown in Table 4.1. The simulation model presented here is a bistatic configuration containing one receiver so multistatic response needs to be simulated in several phases. *Signal generator* block corresponds a radar transmitter generating all the necessary signals needed for signal transmission and coherent reception. The IF-reference and the variable reference go through the *propagation delay* which produces a fixed propagation delay for references. This represents the delay due to the transmission of the references between different sites in bistatic or multistatic configuration. The variable reference also goes through the interference and noise block where errors can be added to the signal to model the propagation path. Hence, in the example simulation configuration presented interferences are added only to this reference while keeping IF-reference clean. An embedded MATLAB function *signalDelay* represents a propagation delay for the transmitted radio wave signal, as well as a target model by calculating the superposition of the reflected signals from multiple point scatterers forming a target. *Downmix* and *IQ-detector* blocks form the receiver, consisting of mixers, filters, and the detector. Generated IQ-samples are then stored for processing in MATLAB.

Table 4.1: *Top level block diagram signals.*

Signal	**Purpose**
Signal generator	
if ref r	Intermediate frequency reference (real sine signal)
var ref c	Variable frequency reference (complex sine signal)
sig trig	Generates rising edge in the beginning of a pulse
sig phase	Continuous phase signal (range $-\pi...\pi$)
clock	Running simulation time (in seconds)
Downmix	
ref in r	Variable reference signal input (real)
sig in r	RF-signal input (real)
out r	Output at IF (real)
IQ-detector	
ref in r	IF-reference signal input (real)
sig in r	IF-signal input (real)
out c	I and Q outputs combined as a complex signal

Signal Generation

Signal generation is actually performed in two blocks. The *Signal generator* block generates reference, or synchronization, signals for coherent reception and control signals for pulse generation which is located in *Propagation and target model* block due to practical reasons explained in Section 4.1. The block diagram of the signal generator is presented in Figure 4.2 and signals and blocks in Table 4.2. The block outputs from top downwards are: simulation time (*clock*), real IF reference (*if ref r*), complex variable reference (*var ref c*), RF signal phase (*sig phase*), and pulse trigger (*sig trig*). RF-pulse is generated outside the signal generator in *Propagation and target model* using the latter two signals.

All signals are derived from the fundamental frequency ,which determines the frequency resolution of the signals generated, and are integer multiples of the fundamental clock frequency. This corresponds stable low frequency local oscillator and frequency synthesizers in radar although phase-locked loops or synthesizers have not been modeled. Signals are derived using complex sine waves and exponential functions together acting as an ideal mathematical phase-lock. This maintains the same phase relative to the fundamental clock signal in every pulse burst when changing the carrier frequency. Without the preservation of the phase relations, meaning all the frequencies in a stepped frequency waveform remaining coherent, a different phase at every pulse burst would be generated destroying the construction of the down range in inverse Fourier transform.

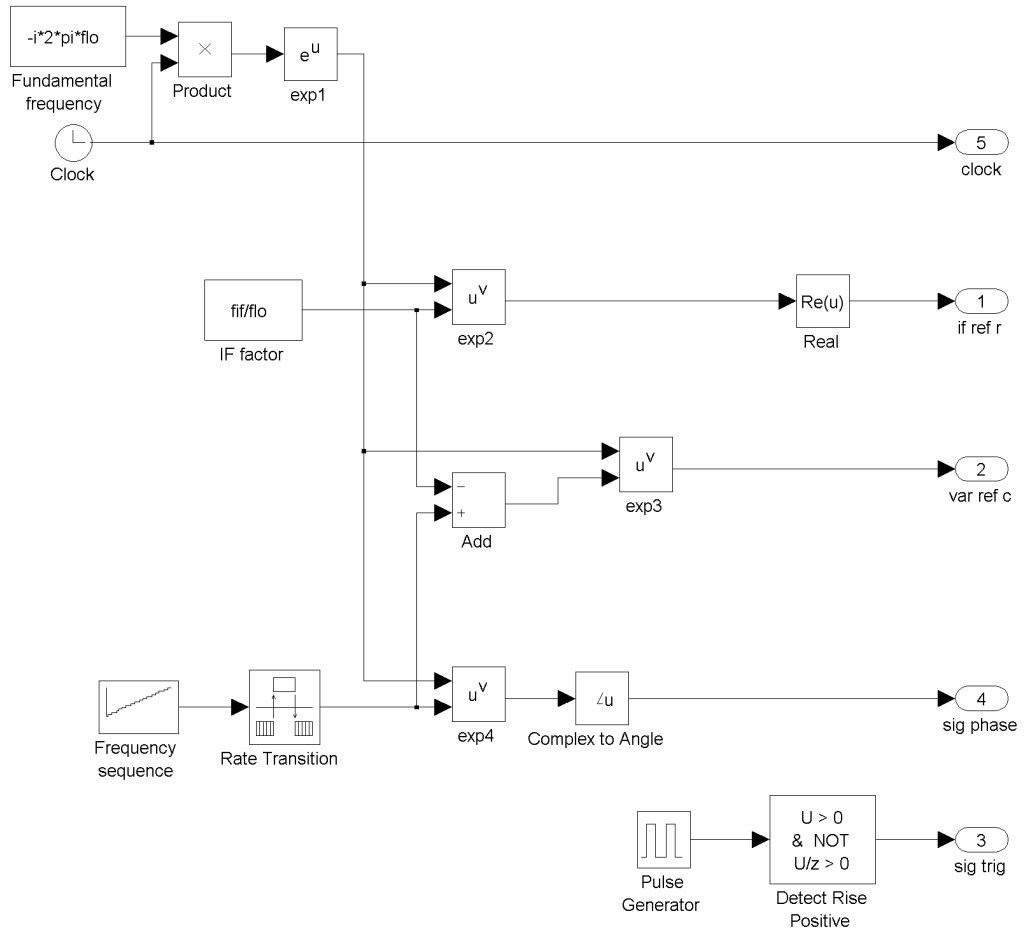

Figure 4.2: *The block diagram of the signal generator. Output signals are listed in Table 4.1. Inputs in the inner blocks are denoted with symbol u and v. For example with the inputs of the exp4 block, u is the output of the exp1 and v is the output of the Rate transition.*

The intermediate frequency reference signal *if ref r* can be derived from Figure 4.2

$$r_{\mathrm{if}}(t) = \mathrm{Re}\left(e^{-\mathrm{j}2\pi f_{\mathrm{lo}} t \frac{f_{\mathrm{if}}}{f_{\mathrm{lo}}}}\right) = \mathrm{Re}\left(e^{-\mathrm{j}2\pi f_{\mathrm{if}} t}\right). \tag{4.1}$$

Similarly the variable reference signal *var ref c*

$$r_{\mathrm{var}}(t) = e^{-\mathrm{j}2\pi f_{\mathrm{lo}} t\left(\frac{f_{\mathrm{c}}}{f_{\mathrm{lo}}} - \frac{f_{\mathrm{if}}}{f_{\mathrm{lo}}}\right)} = e^{-\mathrm{j}2\pi (f_{\mathrm{c}} - f_{\mathrm{if}}) t} \tag{4.2}$$

where $\frac{f_{\mathrm{c}}}{f_{\mathrm{lo}}}$ is the output of the *Frequency sequence*. *Rate transition* block is not taken into consideration because it is needed only due to simulation reasons in Simulink between blocks of different sampling frequencies. Intermediate frequency is constant even if transmitted frequency f_{c} is varied. In such case the variable reference changes so that the demanded transmitted frequency is the sum of the reference frequencies, $f_{\mathrm{c}} = f_{\mathrm{if}} + f_{\mathrm{var}}$. Both reference signals are derived from the LO-signal and phase-lock is achieved by raising this complex signal into the power of required constant.

Table 4.2: *Top level block diagram signals.*

Constant	**Purpose**
flo	Frequency of local oscillator
fif	Intermediate frequency
Block	**Purpose**
Fundamental frequency	Together with *Product* and *exp1* generates the local oscillator signal $e^{-i2\pi f_{\mathrm{lo}}}$
Clock	Running simulation time (in seconds)
IF factor	Integer $f_{\mathrm{IF}}/f_{\mathrm{lo}}$, used to multiply f_{lo} to generate f_{IF}
Frequency sequence	Generates the factor to multiply f_{lo} to generate desired f_{c}. Factor changes after PRI if multiple values of f_{c} are used, thus generating a sequence.
Rate transition	Inner Simulink block needed between two block with different sampling frequency.
Pulse generator	Generates pulse train based on given PRF and pulse width values.
Detect rise positive	Output is *high* on the rising edge of the input and otherwise *low*.

Radio wave signal to be transmitted is not generated in the signal generator because of simulation time step considerations explained in 4.1. Instead, control signals for generating the pulse train are generated. Instant phase output

$$\phi_{\mathrm{s}}(t) = \mathrm{Arg}\left(e^{\text{-j}2\pi f_{\mathrm{lo}} t \frac{f_c}{f_{\mathrm{lo}}}}\right) = \mathrm{Arg}\left(e^{\text{-j}2\pi f_{\mathrm{c}} t}\right), \tag{4.3}$$

bounded between $-\pi$ and π, of *sig phase* and trigger of the rising edge of the pulse *sig trig* along with the *clock* are used in the embedded code block *Propagation and target model* block to generate the RF-pulses.

Reference Signal Transmission

Complex variable reference signal *var ref c* is fed into the *Interference and noise block*, seen in Figure 4.3, where noise and interferences can be added to the signal to model the propagation path. In the simulation presented, interferences are only added to this variable reference signal but only to make the amount of variables smaller. The block can be just copied to the propagation path of the *if ref r* as well if needed. The *Interference and noise* block can generate gaussian and uniformly distributed amplitude and phase noise, and frequency and amplitude modulations. The blocks illustrated in Figures 4.4a and 4.4b perform the noise generation and

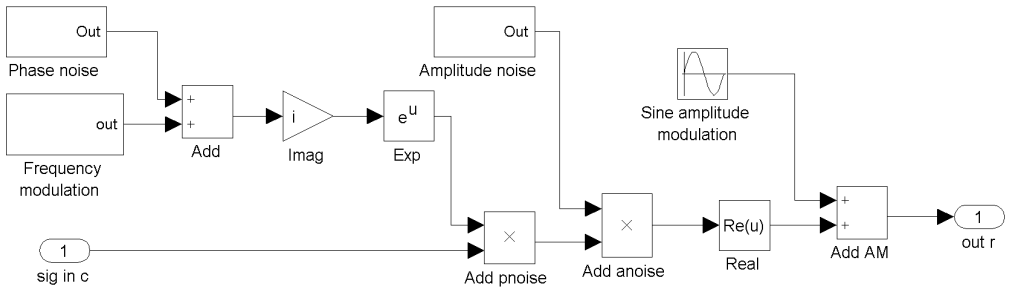

Figure 4.3: *The block diagram of the interference and noise block.*

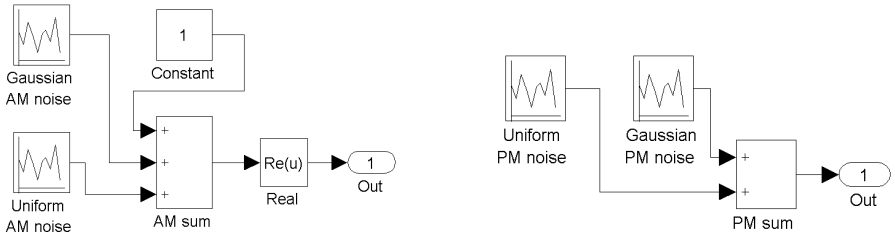

(a) *Amplitude noise.* ***(b)*** *Phase noise.*

Figure 4.4: *Generation of noise inside the interference and noise block. The noise can be shaped to a specific type by using filters in the noise path.*

Figure 4.5 presents the model for frequency modulation. Amplitude modulation is generated by using a plain sine wave generator seen in Figure 4.3.

The input is a complex signal to allow the addition of theoretical phase noise. Correspondingly, amplitude noise only affects the magnitude of the complex signal. In practice, the amplitude and phase components of the noise may be inseparable because the signal in which they emerge is real as is also the output signal of the *Interference and noise* block. However, the model discussed here enables the components to have different characteristics. Phase noise often has a specific spectrum shape, especially true for oscillators where amplitude noise can be insignificant, therefore an accurate model can be created by using filters in the phase noise path.

The implementation of the Frequency modulation block can be seen in Figure 4.5 generating a signal

$$\phi_{\mathrm{FM}}(t) = \mu_{\mathrm{FM}} \sin\left(\omega_{\mathrm{FM}} t\right) \tag{4.4}$$

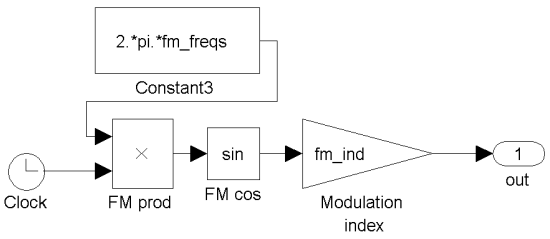

Figure 4.5: *Frequency modulation in the interference and noise block.*

where μ_{FM} is the modulation index and ω_{FM} the modulation frequency. Signal (4.4) represents a varying phase signal which is added to the phase noise $\phi_{\mathrm{n}}(t)$ in *Interference and noise*, resulting in

$$p_{\mathrm{n}}(t) = e^{-\mathrm{j}(\phi_{\mathrm{n}}(t)+\mu_{\mathrm{FM}}\sin(\omega_{\mathrm{FM}}t))} \tag{4.5}$$

before *Add pnoise* block in Figure 4.3. This is multiplied with the input signal which is the signal (4.2). Substituting $\omega_{\mathrm{var}} = 2\pi(f_{\mathrm{c}} - f_{\mathrm{if}})$ for simplicity

$$p(t) = e^{-\mathrm{j}\omega_{\mathrm{var}}t}e^{-\mathrm{j}(\phi_{\mathrm{n}}(t)+\mu_{\mathrm{FM}}\sin(\omega_{\mathrm{FM}}t))} = e^{-\mathrm{j}(\omega_{\mathrm{var}}t+\phi_{\mathrm{n}}(t)+\mu_{\mathrm{FM}}\sin(\omega_{\mathrm{FM}}t))}. \tag{4.6}$$

Amplitude noise $a_{\mathrm{n}}(t)$ with mean value of 1 is added to the signal and the real part of the result is taken. Finally amplitude modulation of frequency ω_{AM} and modulation index μ_{AM} can be added with the sine generator. Thus, the output *out r* of the *Interference and noise* can be written as

$$s(t) = [1 + \mu_{\mathrm{AM}}\sin(\omega_{\mathrm{AM}})]\,\mathrm{Re}\left[a_{\mathrm{n}}(t)e^{-\mathrm{j}(\omega_{\mathrm{var}}t+\phi_{\mathrm{n}}(t)+\mu_{\mathrm{FM}}\sin(\omega_{\mathrm{FM}}t))}\right]. \tag{4.7}$$

Certainly, if error and interference sources are set as zero the *Interference and noise* block passes the input signal directly without any distortions.

Target Model

Target model is realized using embedded MATLAB function block containing code optimized for Simulink use. For the sake of efficiency, these functions are compiled before executing so there are constraints on the code to make compiling possible. High efficiency is needed since the function is executed on every simulation step.

A target for a simulation is created using a group of point scatterers. Each point has a specific location in space and RCS value. By using sufficient amount of points, more complex targets can be created. The simulation calculates the reflections caused by individual scatterers and sums them to form the superposition response. The location of the particle causes corresponding delay. The modeling of the target itself, the group of points, is not a topic here so the simulation tool operates with pre-processed matrices which contain the location and RCS of point scatterers in a function of time, in fact in a function of discrete PRI steps. The task to make points moving is not difficult but how RCS changes requires more consideration.

Since computer simulation is always a discrete process and the time delay accuracy for proper phase reconstruction is rather high, the implementation needs some special attention. Simulation is executed by calculating the system variables and states at discrete time steps, simulation steps, which are the fundamental time units of the simulation. Since these are the smallest possible time unit in the simula-

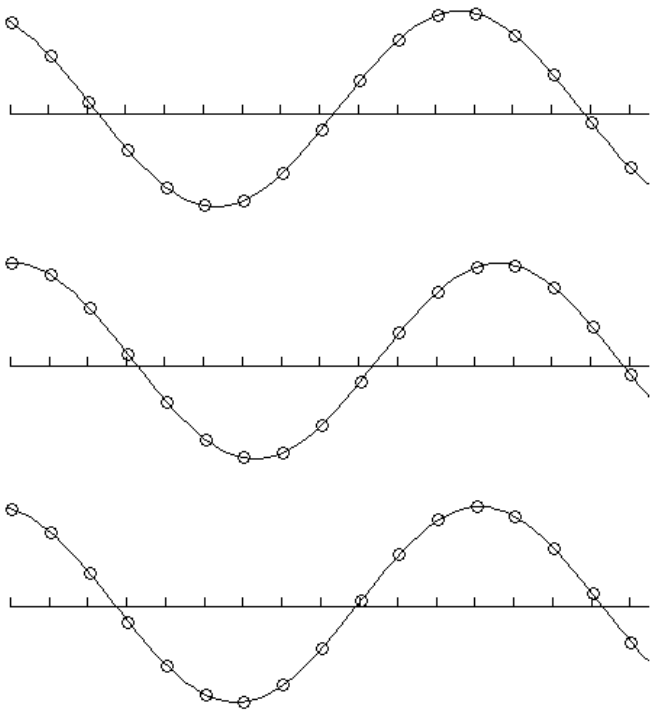

Figure 4.6: *Circles represent the sampling instants of the signal. Signal in the middle is the uppermost delayed by one sample. The undermost signal is the uppermost delayed by half a sample, implemented by resampling the signal.*

tion model, it arouses some constraints. When delaying the transmitted signal in *Propagation and target model* block, based on the length of the propagation path of the pulse train, the smallest possible discretization step of the delay equals the simulation step. Because the fundamental sampling frequency, the reciprocal of the simulation step, is 5-10 times the highest frequency in the system, one simulation step equals tens of degrees in the radio frequency signal phase. In a simulation where interferences causing one degree error are to be examined, the delay adjustment in that way is too coarse.

To overcome this problem the signal can be resampled and the sampling points can be chosen so that the required delay is an integer multiple of the simulation step. An example can be seen in Figure 4.6. However, resampling is too slow process to do accurately at every simulation step. In a simulation environment, with some assumptions, the problem can be solved by generating the signal using the convenient sampling instant in the delaying point of view. Since the needed delay is known and the initial phase of the generated signal can be obtained from the *Signal generator* block, the signal can be generated so that the needed delay is an integer multiple of the simulation step. So, after all, the delay in total consists of an integer multiple of the simulation step as a coarse delay adjustment and the phase shift which is the fine adjustment of the delay. This method allows for very accurate

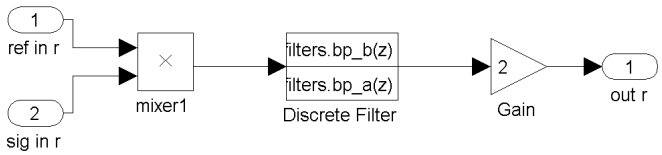

Figure 4.7: *The block diagram of the downmix from radio frequency to intermediate frequency.*

setting of the delay. As a summary, instead of delaying the signal it is actually created when the needed delay has already passed, using the delay and initial phase information. As a result, when using sine wave signal, the target model output signal corresponds exactly a delayed version of the transmitted signal. This can also cause limitations, for example, if oscillator errors, which affect both transmitted and reference signals, are to be modeled in the future.

Downmixing and Detection

The first stage of the signal reception is the downmixing of the RF pulse train into the intermediate frequency (IF). This is done using a mixer, as can be seen in Figure 4.7. Mixer produces sum and difference components of the frequencies fed to it. Since on reception the signal needs to be downmixed the higher component is filtered out. Thus a band-pass filter centered at IF follows the mixer. The filter bandwidth must be wide enough to pass the signal without significant attenuation but narrow enough to considerably attenuate the image frequencies and excessive noise. The gain stage compensates the loss of power when filtering out the image frequencies. Filter type on Simulink is discrete filter due to the fact that signals are discrete digital signals sampled at every simulation step.

The received signal is detected to baseband frequencies using 2-channel IQ-detector, see block diagram in Figure 4.8. The downmixed IF-signal is mixed with the IF-reference and the 90° delayed version of the IF-reference to generate baseband I and Q signals. I and Q samples are combined to form one complex sample. The complex signal is then fed to a low-pass filter to filter out the higher image frequencies and amplified to compensate the power loss.

In detector signal needs to be delayed exactly 90°, so similar problem arises as in delaying the pulse, explained in Section 4.1. Here resampling is not even acceptable mean since it would modify the signal while it should be an identical delayed copy of the reference used for the I-channel detection. However, the delay is always constant in phase and also in time because IF is constant even if the carrier frequency is changed. Hence, in fact the simulation step for the whole simulation is chosen so that the 90° in IF is an integer multiple of the simulation step. This can be done because there is nothing that requires some exact time for the simulation step. In

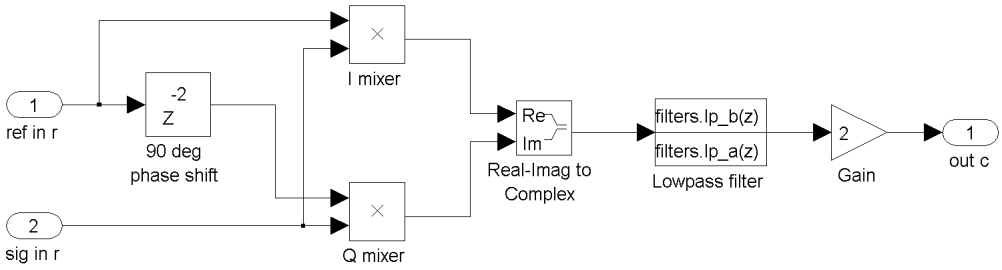

Figure 4.8: *The block diagram of the IQ-detector.*

the test simulation and in Figure 4.8 the delay is 2 simulation steps.

4.2 Non-Ideal Models

Despite the promising platform for real-life imitating simulations is achieved, considerable amount of work is still needed to get reliable results since most parts in the simulation are modeled as ideal components using only mathematical formulae. Models need to be modified to contain at least typical characteristics and errors to be able to compare the simulation results to practical devices. This is challenging since it is difficult to gain information on the components used in radars, thus, only guesses could be made without further information. In this Section some typical errors to concentrate on in the future are given. Every block in the block diagram in Figure 3.1 has some typical errors, nonlinearities, or other undesired effects on the signal. Many of them are insignificant and covered by more dominant ones, however, eventually noise and nonlinearities set the performance limits for the system. The motivation to extensively model and analyze these errors is to gain knowledge what are the dominant noise and error sources on the system and how they affect the performance.

Oscillators

Oscillators are essential components in radar so their errors are also important. Usually radar has one stable local oscillator as a basis for other oscillators and timing circuits. In Section 3.6 oscillator output voltage was modeled as $V(t) = (V_0 + \epsilon(t))\sin(2\pi f_0 + \phi(t))$ with amplitude noise $\epsilon(t)$ and phase noise $\phi(t)$. In high-performance sources amplitude noise can be neglected while phase noise is the dominant noise, especially other than local oscillator. Skolnik states that when state-of-the-art local oscillator is used, the phase noise of other oscillators along with timing jitter of the AD-converter are the dominant performance limiters [20, p. 6.15]. While in the real world the amplitude and phase noise components can be inseparable, they usually have different characteristics. While general noise floor is usually flat white noise, in frequency sources phase noise increases when moving

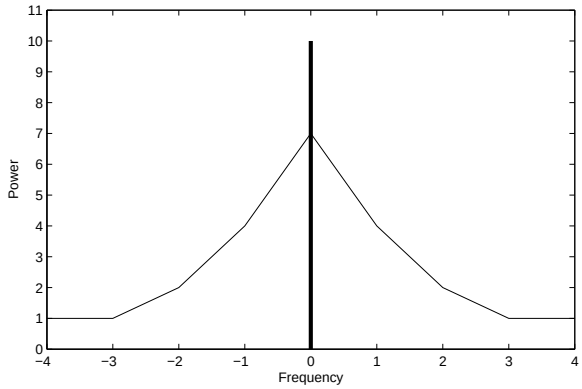

Figure 4.9: *Idealized oscillator spectrum. Phase noise concentrates around nominal frequency being much higher than the noise floor elsewhere. [10, p. 362]*

closer to the carrier. In Figure 4.9 is a theoretical example of phase noise curve around the nominal frequency spike. The noise grows with increasing power when getting closer to the output frequency. In the simulator noise can be shaped by adding filters with desired transfer functions in the noise path. [10, pp. 345-365], [20, p. 6.14-6.20]

Besides noise and wide-spectrum interferences, slower changes in phase or frequency occur in oscillators. In monostatic radar this causes phase or frequency mismatch at the reception due to the instability in oscillator during the pulse propagation, thus the stability requirement is typically related to the flight time of the pulse, or the maximum range of the radar. The changes between the pulses matter and the absolute error cancels out [17]. In multistatic radar the effect depends on the synchronization scheme. If the reference is transferred from the transmitter the effect of oscillator drift decreases since it is the propagation time difference between direct RF-signal and transferred reference which matters. However, the reference propagation path adds its own effects on the signal. In case of independent clock systems at receiver sites all the drifts and errors may accumulate. The requirements are so high that at least periodical synchronization is needed via some external signals. From the simulation standpoint it is simpler to start with the transferred reference scheme. This can be modeled using the interference model presented in the simulation tool at the moment, and if oscillator errors are added as well propagation delay should be modeled. In practice oscillators also encounter drifts, where the time scale can be from seconds to years, due to changes in supply voltage, temperature, humidity, and component aging. [17], [10, p. 399]

Another characteristic present in oscillator are the spurious outputs. They can be divided into harmonic, which are the integer multiples of the nominal frequency, and nonharmonic spurious signals. It is also worth noticing that the spurious components show increased phase noise around them similar way as the phase noise increases

nearby the nominal frequency. At least harmonic components are always present in practical systems due to the system nonlinearities but their levels can be affected by careful design. Also they can be considered in the overall system after the oscillator by using frequency translation and filtering schemes so that the strongest and most disruptive components do not affect system performance too much. [10, pp. 395-399]

Frequency synthesizers are used after the stable oscillator to provide desired frequencies. Techniques such as phase-locked loops (PLL), direct digital synthesizers (DDS), or digital upconverters (DUC) can be involved. It is difficult to know the characteristics of the synthesizer without exactly knowing the used devices. They affect the overall phase noise, and as was stated above, when state-of-the-art local oscillator is used, they in fact determine the phase noise of the system and have major role in the performance as a whole [20, p. 6.15]. This can be also used as a guideline in simulation. [10, pp. 408-417], [20, pp. 6.47-6.51]

Mixers

Mixer has 2 input ports and an output port. Desired mixer output signals are sum and difference of inputs but in reality the output $f_{out} = \pm nf_1 \pm mf_2$. Although the power decreases when the order increases, mixer generates plenty of undesired frequencies which need to be filtered. Interport isolation is also imperfect which leads to the leakage of input signals to the output port without frequency translation. An example of the power of the components in one particular mixer is shown in Table 4.3. Values are the power below the carrier, and they depend on the input power level and frequency so the presented table is only an example, however, it can be a typical case. In practice the power level need to be optimized for the ports to generate desired outputs but no more unwanted signals than necessary. Mixer also causes some attenuation, or conversion loss. Frequency translation schemes need to be designed so that leaking signals and spurious components can be easily filtered or otherwise do not significantly weaken the performance. In simulation it would be necessary to add the strongest spurious components. If the frequency translation scheme is to be designed in the simulation tool, more detailed modeling may be necessary. [10, pp. 263-306], [20, pp. 6.10-6.14]

Mixers can be also realized in several ways. Types of mixers are for example single-ended mixer, single-balanced mixer, and double-balanced mixer. Various types have their own characteristics in interport isolation and spurious components, and also the port impedances differ significantly. However, in simulation environment the types may not need to be considered otherwise if the effects are included in the port isolation and spurious parameters. For more detailed modeling of impedance mismatch and loading effects, the implementation need to be known very precisely. [10, pp. 313-337]

Table 4.3: *Power of spurious components in dB below the desired output ($m = n = 1$). Table is example of one particular mixer with $f_{\mathrm{RF}} = 500\ MHz at -4\ dBm$, $f_{\mathrm{LO}} = 470\ MHz at 7\ dBm$, and output $f_{\mathrm{IF}} = 30\ MHz$ measured to be $-11\ dBm$. Frequencies and power levels affect the spurious outputs. [10, p. 305]*

		RF harmonic (n)					
		0	1	2	3	4	5
LO Harmonic (m)	0		17	43	44	76	66
	1	32	**0**	60	34	68	75
	2	23	39	45	49	56	67
	3	36	17	56	35	72	53
	4	43	33	51	49	56	57
	5	35	37	60	36	61	48

AD-Converters

A component which is getting more important in radar is the AD-converter. All the demanding processing is made digitally so ADC accuracy affects the processing. The requirements are also getting higher because the signal bandwidth is growing and a trend is to move ADC closer to the antenna, for example, sample at IF and perform detection digitally. The advantage is that some of the errors mentioned above disappear or become more predictable and constant when the operations are made digitally. On the other hand, the ADC errors become more dominant. [20, p. 2.78, pp. 6.35-6.40]

ADC has many types of undesired effects and performance figures and only some of them are listed here. More comprehensive explanations can be found in [1] and [20, pp. 6.35-6.40]. First of all the converter also needs stable and pure clock signal as some other parts of the radar. Phase noise, or clock jitter as it is often called in clock signals, causes uncertainties in sampling instants which causes distortions and noise in the digitized signal. This becomes particularly important when fast sampling rate wide-bandwidth converters are used and the input signals have rapid rise and fall times. Even tiny drift in sampling instant results in rather different amplitude value than it should be. [1]

Digital signals have finite amount of possible amplitude values, for example 16-bit converter has $2^{16} = 65536$ levels, so AD-converters quantize signal. This causes white quantization noise, whose amplitude is uniformly distributed between $-LSB/2$ (Least Significant Bit) and $LSB/2$, depending on the number of quantization bits since it determines the magnitude of the LSB. For the quantization noise of an ideal converter, RMS value of $LSB/\sqrt{12}$ can be derived as well as the theoretical maximum SNR,

$$SNR_{\mathrm{ideal}} = 6.02n + 1.76 \tag{4.8}$$

where n is the number of bits in the conversion. Practical AD-converters are not perfectly linear, especially the high-speed converters used in radar. Heavily upsampling serial-type delta-sigma-converters have excellent linearity but they are applicable only in audio frequencies. In high frequencies parallel-type or pipelined converters need to be used and some nonlinearity occurs. Linearities are expressed as differential and integral nonlinearities with unit LSBs. Due to the nonlinearities the effective resolution and SNR are worse than the number of the bits states. Thus, the effective number of bits (ENOB) is often expressed for the ADC. Furthermore, in order to get most out of the ADC the input signal should be scaled so that it covers the whole dynamic range effectively, still preventing saturation. However, due to the extensive dynamic range of radar it is not easy. [20, pp. 6.35-6.40], [1]

Internal nonlinearities of ADC also generate new frequency components similarly as mixers. These can be categorized as harmonic distortion and intermodulation distortion depending on the dependence of the new components to the input components. Due to these distortions above noise floor it is necessary to define another figure similar to SNR. SINAD (Signal-to-Noise-and-Distortion Ratio), or SNR+D, instead, compares the signal to the strongest distortion and is expressed in decibels to carrier (dBc) or decibels scaled to the full-scale output of the ADC (dBFS).

Other Components and Issues

Amplifiers amplify signal or operate as impedance transformers and they exist in various parts of radar. In practice, account should be paid that they always work in their linear operating range which can be sometimes difficult in radar due to the very high dynamic range. Actively changing attenuators are thus also needed in radars. Amplifiers can affect the noise level and bandwidth of signals. Filters have the same effects and also exist in several parts of radar. They are used to restrict the bandwidth to filter out undesired spectral components, such as mixer image frequencies or above-Nyquist frequencies in antialiasing filter, or noise to increase SNR. Analog filters can be imitated using IIR filters in simulation but digital filters are usually FIR-type due to their phase linearity. [20, pp. 6.24-6.29]

Another general issue in radar is the channel mismatch between I- and Q-channels. The analog parts of the two channels are never perfectly identical. One of the reasons that digitalization is moving closer to the antenna when AD-converters evolve is to have more digital parts where channels are identical, as well as do not suffer as much from environmental variables as their analog counterparts. This can be modeled using gain, phase, or frequency response imbalance. [20, pp. 6.32-6.35]

Radar receiver on the whole has many sources of noise since all components have finite noise level. However, according to Skolnik [20, p. 6.5], AD-converter noise typically dominates the overall noise in radar, although, the development of

the converters have to be considered. However, it is known that the quantization noise sets the theoretical noise limit of the ADC, the practical noise being closer to the one calculated using effective number of bits. Another noise which can be dominant is due to clock jitter, $SNR_{\mathrm{j}} = -20\log_{10}(2\pi f\sigma_{\mathrm{j}})$, σ_{j} being the jitter RMS value, [20, p. 6.40]. These can give guidelines for the noise level if nothing else is known. When noise level has been determined, signals need to be scaled to correspond maximum signal levels in radar and make sure they stay within the limits in simulation. Otherwise things go easily wrong with the enormous dynamic range of the 64-bit floating-point numbers in MATLAB.

Not all significant error sources have been listed here. If the external electromagnetic background and clutter is somehow modeled, radar antenna can receive remarkable signal power which may cause errors or saturation in the receiver. Antenna motion also causes distortion to the signal in the form of amplitude and phase modulation due to the antenna scan.

It can be seen that considering the undesired effects of components even in very general level gives many variables and uncertainties. Carefully modeling and verifying these effects requires time. Not only the effects need to be modeled in the simulation tool but the parameters need to be known as well. Thus, it also requires knowledge of the typical components used in radar or exact component types used in some application, which is unlikely. By expanding the simulation model to cover the presented errors creates comprehensive simulation system. However, the simulation time will drastically suffer. It can be necessary to perform more analysis among the interferences to learn which are insignificant and can be neglected to make simulation simpler. After all, that enhances the knowledge of which errors are dominant in the system.

4.3 Moving Target Indication

Moving target indication (MTI) is a simpler mean than pulse Doppler processing to distinguish moving targets from ground clutter caused by terrain, such as buildings, masts, trees, and hills. In its very basic form delay line is used and the consecutive pulses are subtracted from each other. In theory, stationary target produces identical response from pulse to pulse, so subtracting results in zero, while moving target produces Doppler shift and hence consecutive pulses differ, resulting in nonzero residual signal. Thus, MTI acts as a high-pass filter and the shape of the response depends on the type of the implementation, such as order of the delay line. MTI only distinguishes moving targets from stationary objects without any further information, such as velocity. Due to that pulse Doppler processing has replaced MTI in many applications. [20, pp. 2.2-2.19]

In practice pulses reflected from a stationary object are not perfectly identical

due to interference, noise, and instabilities of the radar. Instability is referred to the slight fluctuations in phase and frequency in the reference oscillator of the radar, thus, what is to be modeled in the simulation. The effects on the Doppler processing and how they can be seen on the result signals are more complex issues. When using stationary objects and examining the MTI performance, some key figures connected to the stability can be developed. This approach is used when analyzing the various reference signal distortions in the results of this work, in Section 5.2.

Noise and some level of nonlinearity are always present in a real device but in simulator interferences can be excluded if wanted. In simulation software, the only restricting factor is the inaccuracy caused by discrete time operation and finite bit depth. However, this is well beyond the noise level of a practical application and thus can considered as noise-free case. Therefore, if a relation between the interference in reference signals and MTI-figures can be established, these can be used as performance figures in simulations.

Noise causes random instability and reduces the MTI attenuation. However, FM modulation has a special interest since it can model slow time fluctuation of the oscillator frequency. If this fluctuation is on the order of PRF or faster, variation in phase can be expected thus affecting the MTI performance. In a simulation, the target object can be kept perfectly stationary and thus use the attenuation of the consecutive pulses to analyze the effect of the errors and interferences fed to the system. MTI-system can be implemented in various ways but here only simple pulse canceler is used for the purpose. The attenuation between complex pulses $\mathbf{z}$ can be simply defined as

$$L_{\mathrm{dB}} = 10 \log_{10} \frac{(\mathbf{z}_2 - \mathbf{z}_1)^2}{\frac{1}{2}\left(\mathbf{z}_2^2 + \mathbf{z}_1^2\right)}. \tag{4.9}$$

The role of the MTI-filter design is not considered, although the shape of the frequency response has to be taken into account related to the predominant ground clutter environment within real applications.

5. SIMULATION RESULTS

This Chapter presents functionality of the simulation tool introduced in Chapter 4 and several results achieved using it. The results at the moment show only the operation of the tool and no actual results for the synchronization effects have been gained. To achieve that, an important task is to verify the operation of the tool to ensure it works as the theory implies. Then simulations can be performed using the initial parameters of interest and to get results on how the interferences or other parameters of interest affect on the selected simulation scenario, and eventually derive a relation between the interferences and the end result.

5.1 Simulation Tool Operation

The features of the developed tool are verificated by presenting figures of the signals inside the simulation tool and comparing these signals to the literature and the theory presented, mainly in Chapter 3. The Figures presented are for demonstrating the proper operation of the simulation tool and hence do not necessarily representing any practical results nor parameters. The basic simulation parameters used are in Table 5.1. All the demonstration cases of the tool are briefly defined in Table 5.2.

Signal Generation

The five outputs of the *Signal generator* block, introduced in Figure 4.2, can be seen in Figure 5.1 based on the operating frequencies presented in Table 5.1. The signals from top to bottom, referred to the names in simulation tool shown in Figure 4.1, are *if ref r*, the real part of the *var ref c*, *sig trig*, *sig phase*, and *clock*. The

Table 5.1: *Operating parameters of test simulation.*

Parameter	Value
Radar parameters	
Carrier frequency (f_c)	5 GHz
Intermediate frequency (f_{if})	3 GHz
Variable reference ($f_c - f_{if}$)	2 GHz
PRF	250 kHz
Pulse width	50 ns

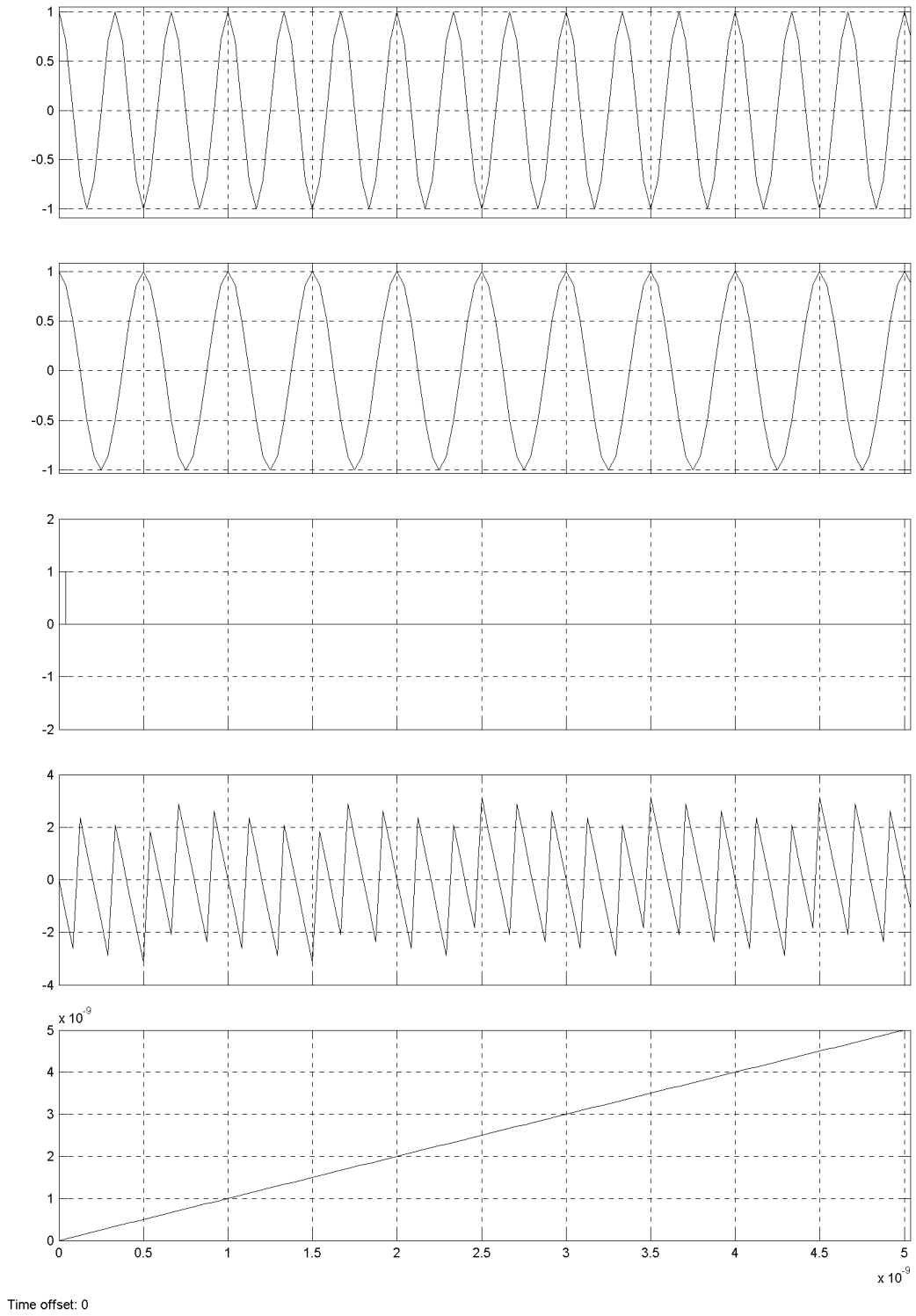

Figure 5.1: *Signal generator outputs in a function of time, from top to bottom: IF reference, variable reference, signal trigger, signal phase and clock.*

Table 5.2: *Noise and interference simulations that show the functionality of the simulation tool. In the 1st run all parameters are mentioned, in other runs only the ones differing from value 0. Reference amplitude is normalized to 1 and no attenuation occurs.*

Parameter	Value
Run 1: Noise-free (Figure 5.2)	
Gaussian amplitude noise variance (mean=0)	0
Uniform amplitude noise limits	0
Gaussian phase noise variance	0 rad
Uniform phase noise limits	0 rad
FM frequency	0 Hz
FM index	0
AM frequency	0 Hz
AM index	0 %
Run 2: Gaussian amplitude noise (Figure 5.3a)	
Gaussian amplitude noise variance (mean=0)	0.01
Run 3: Uniform amplitude noise (Figure 5.3b)	
Uniform amplitude noise limits	±0.05
Run 4: Gaussian phase noise (Figure 5.5b)	
Gaussian phase noise variance	0.01 rad
Run 5: Uniform phase noise (Figure 5.5b)	
Uniform phase noise limits	±0.05 rad
Run 6: Frequency modulation (Figure 5.7)	
FM frequency	200 MHz
FM index	3
Run 7: Amplitude modulation (Figure 5.8)	
AM frequency	600 MHz
AM index	50 %

trigger output generates a short trigger pulse in the beginning of PRI to indicate the *Propagation and target model* block about the time of the pulse generation. Signal phase outputs a wrapped phase varying between $-\pi$ and π which is used to store the initial phase for the pulse generation. Clock is the instant simulation time t used together with the phase to create the sine signal in the *Propagation and target model* block.

Interference And Noise

Interference and noise are generated and added to the variable reference signal in complex form. Table 5.2 defines the parameters of the interference simulations. The

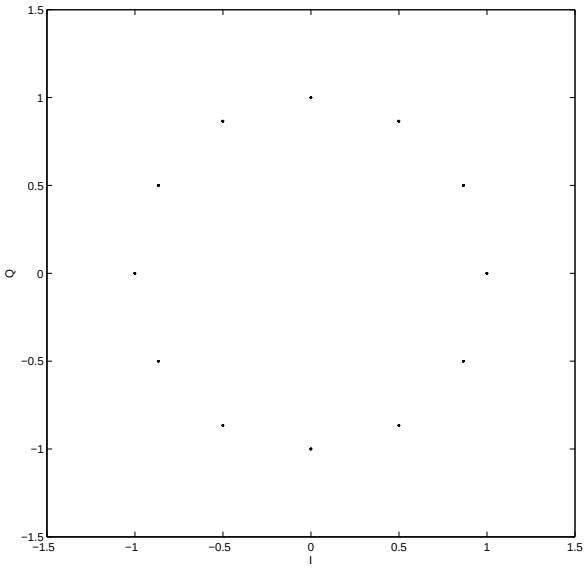

(a) *Complex unit circle. Notice that the samples are at equal phase round by round on the unit circle due to the sample rate being exactly multiple of the reference frequency.*

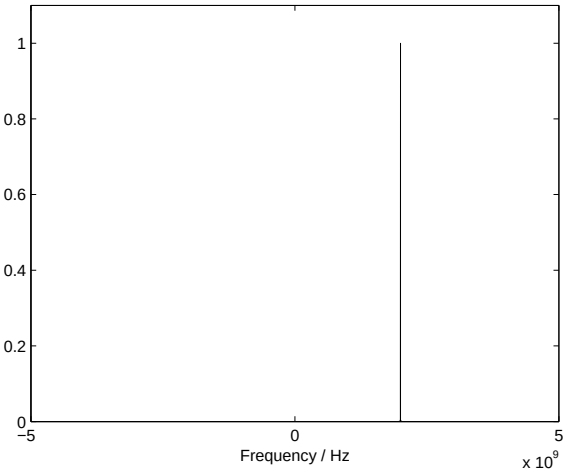

(b) *Frequency spectrum. Complex signal lies only on the right side of the spectrum.*

Figure 5.2: *Noise-free complex reference signal.*

complex reference can be sampled and drawn on the IQ-plane forming a unit circle due to normalized amplitude. Figure 5.2 presents noise-free complex reference signal sampled at every simulation step. Figure shows that the simulation rate is 12 times the reference frequency resulting in 12 points on the unit circle, and samples pile on top of each other round by round on the unit circle due to the sample rate being exactly multiple of the reference frequency and due to the ideal signal. Variable

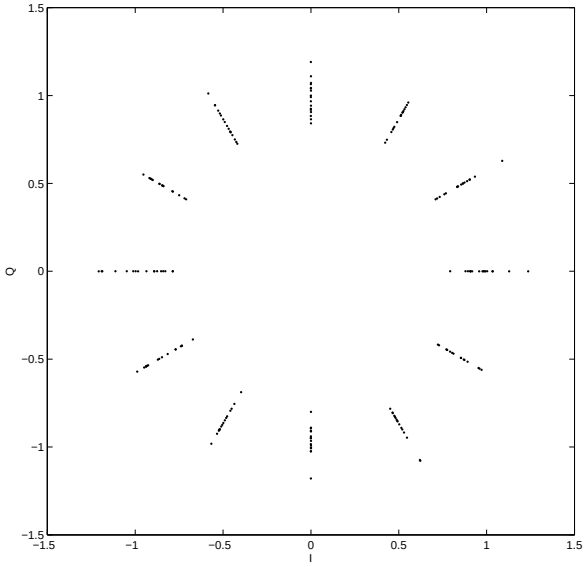

(a) *Gaussian amplitude noise.*

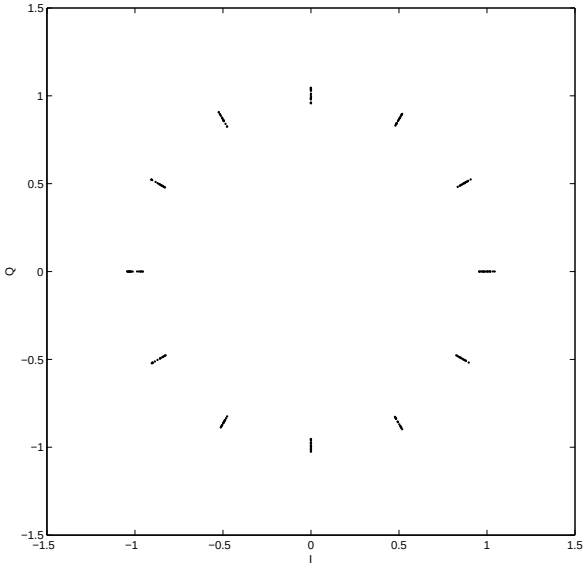

(b) *Uniform amplitude noise.*

Figure 5.3: *Amplitude noise in a complex reference.*

frequency being 2 GHz the simulation rate is then $12 * 2$ GHz $= 24$ GHz which is 8 times the 3 GHz IF-reference. Thus simulation step is 45° of the sinewave period of the IF-reference, as was stated in Section 4.1.

When the theoretical model about the AM and PM noise components, presented in Section 3.6, is used, amplitude noise affects only the amplitude and phase noise only the phase of the sample. Thus, amplitude noise varies the absolute value, or

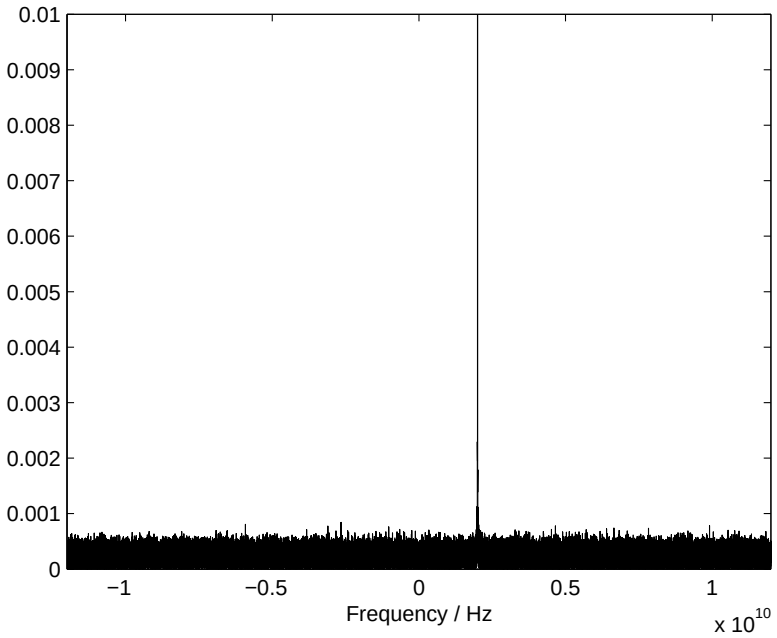

Figure 5.4: *Frequency spectrum of gaussian amplitude noise presented in Figure 5.3a Spike is normalized to 1 and figure is zoomed in to show the level of the noise.*

length of the phasor, and phase noise generates variation on the phase angle.

Gaussian amplitude noise with the mean of 0 and the variance of 0.01 can be seen in Figure 5.3a and uniformly distributed amplitude noise within the limits -0.05...0.05 in Figure 5.3b. The amplitude of the reference signal is normalized to 1 and no attenuation occurs, so the noise values are referred to this. Gaussian phase noise with the mean of 0 and the variance of 0.01 radians can be seen in Figure 5.5a and uniformly distributed phase noise within the limits -0.05...0.05 radians in Figure 5.5b. These values have been also verified by calculating the variance and limits of the sample vectors in MATLAB.

This theoretical separation of noise types into ideal amplitude and phase noise allows generating different characteristics to these noise components, as was mentioned in Section 4.1. However, in practice they add together and the real part of the signal is used in the next phase of the radar system. Figures 5.6a and 5.6b are the noise in Figures 5.3a and 5.5a, respectively, projected in the real axis. The sine wave is drawn to illustrate the instant value of the reference sine signal, and the noise represents the noise variance at the certain point in the sine wave. This representation assumes that the phase (x-axis) progresses linearly and treats the noise as deviation in signal value. Amplitude noise has its maximum variance on the apices of the sine wave but no effect at the zero-crossing. Phase noise has no effect on the apices but on the zero-crossings, thus the noise adds randomness causing uncertainty on the zero-crossing instants.

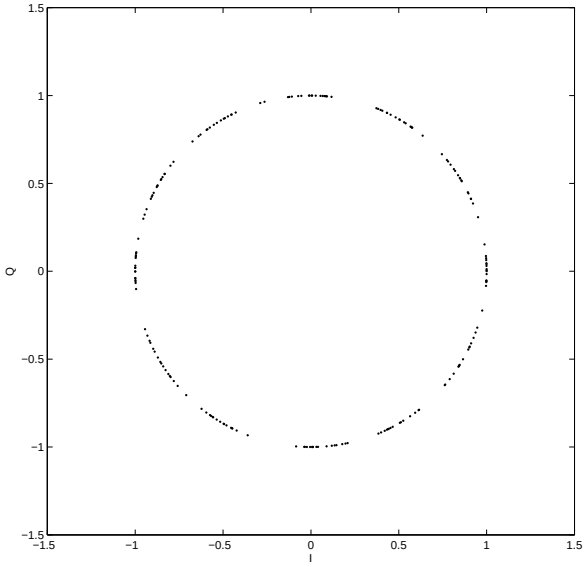

(a) *Gaussian phase noise.*

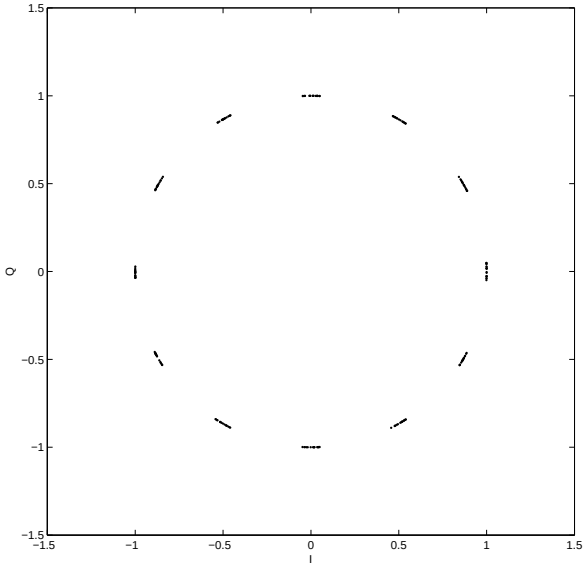

(b) *Uniform phase noise.*

Figure 5.5: *Phase noise in a complex reference.*

The result of the frequency modulation with a modulation frequency of 200 MHz and a modulation index of 3 can be seen in Figure 5.7. The carrier wave modulated by a 600 MHz sine wave with a modulation index of 50 % is presented in Figure 5.8. Values for these modulation examples were chosen to be high enough to obtain visible results. The disturbances should not be at this level in real radar hardware.

All the discussed Figures 5.2–5.8 represent the variable reference signal $s(t)$, for-

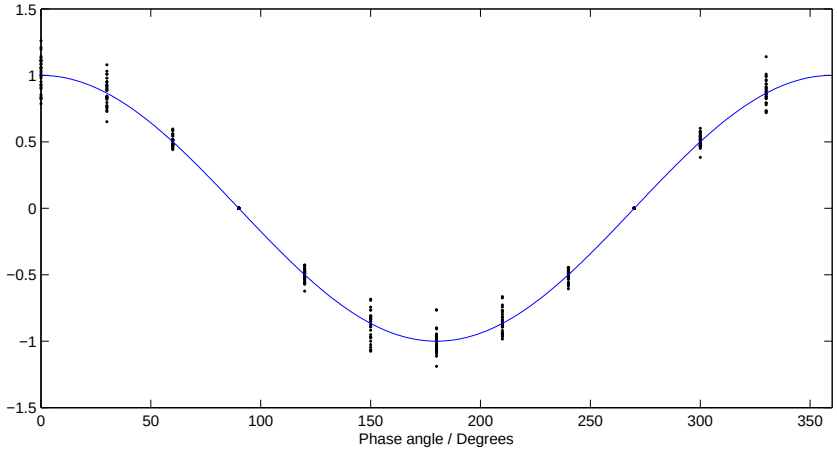

(a) *Real part of the amplitude noise.*

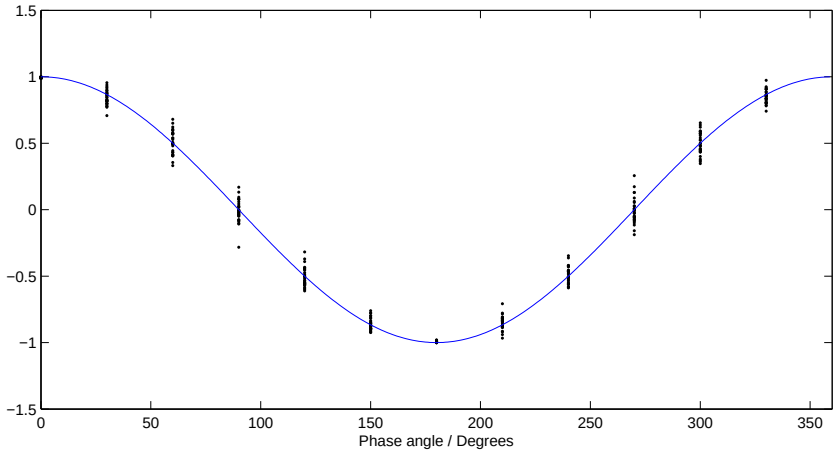

(b) *Real part of the phase noise.*

Figure 5.6: *Noise in a real reference. This representation assumes that the phase (x-axis) progresses linearly and treats the noise as deviation in signal value.*

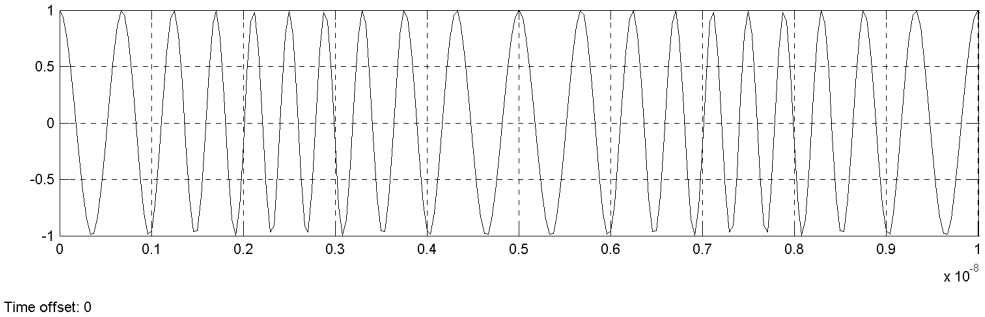

Figure 5.7: *Frequency modulated carrier.*

mulated in Equation (4.7), that is used in the *Downmix* block of Figure 4.1 (*ref in r*) to shift the received radio frequency signal to intermediate frequency. *Interference and noise* block (Figure 4.1) with *Propagation delay 2* determine the disturbances

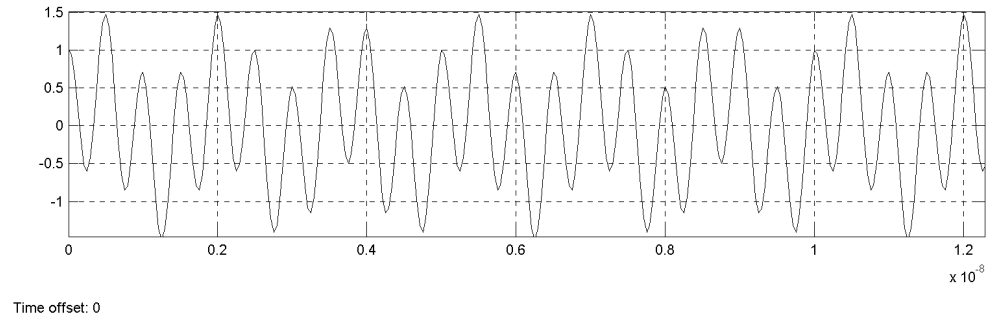

Figure 5.8: *Amplitude modulated carrier.*

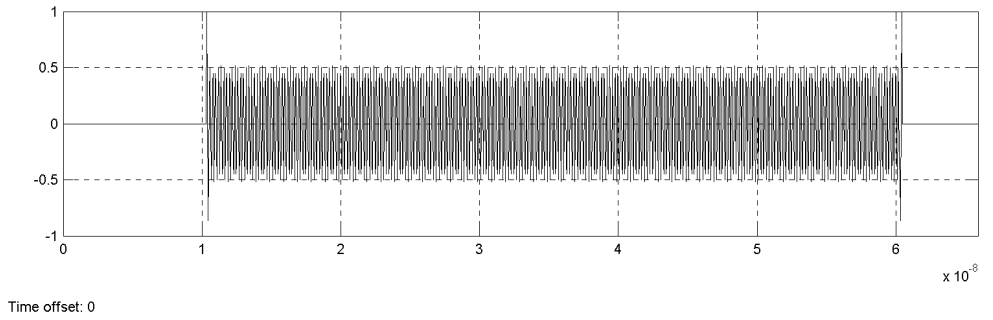

Figure 5.9: *The sum of two reflections. Notice the spikes at the beginning and at the end due to a small propagation delay difference of the two superposed echoes.*

in the simulation model. Thus $s(t)$ is the signal in which there is described the effects in the transmission path of the reference. The reference of adequate quality provides a coherent multistatic radar. The main idea of the synchronization study discussed in this document focuses on the effects caused by the disturbances in $s(t)$ on the coherent response aquisition.

Propagation and Target Model

In this demonstration example, the target consists of two point scatterers with the total propagation distances of 3.1 m and 3.125 m the carrier frequency being 5 GHz. Short distances have been selected to keep simulation time short, and because the purpose is only to demonstrate the effect of superposition due to the difference in distance. Furthermore, the amplitude is normalized so no propagation or RCS attenuation occur. The propagation delay of 3.1 m / c = 10.4 ns can be seen in Figure 5.9 indicating a correct delay calculation. Since the difference between the scatterers is almost a half wavelength, an attenuation of the sum signal occurs. There are spikes in the beginning and the end of the sum pulse because of the slight time difference and an accurate superposition method.

Downmix and Detection

Figure 5.10 presents the signals related to downmixing and detecting in the time domain and 5.11 in the frequency domain. The delayed pulse with carrier frequency of 5 GHz (the first signal in Figure 5.10) is multiplied with the 2 GHz variable reference (the second signal in Figure 5.10), thus generating the sum and the difference components of the two signals. The higher 7 GHz component is filtered out with a bandpass filter and the remaining 3 GHz component is presented as the third signal in Figure 5.10. This signal also goes through an amplifier with a gain of 2.

After downmix the two signals are fed to the IQ-detector which multiplies the pulsed signal with the reference of and the 90 degree delayed version of the reference, generating I and Q signals. Since the downmixed signal has the same frequency, after another low-pass filter the detector generates two baseband signals, seen as the two last signals in Figure 5.10, again amplified by 2.

5.2 MTI-Attenuation

The effect of AM on MTI depends on the parameters of the radar. If the frequency of AM is small compared to the pulse width, amplitude variations within a pulse are insignificant. Amplitude variations from pulse to pulse affect MTI performance and thus it strongly depends on the AM frequency to PRF ratio. Furthermore, the strength of the modulation, modulation index, also affects the results.

The effect of AM on MTI is largest when the AM frequency is half of the PRF, or $f_{\mathrm{m}} = \frac{1}{2} f_{\mathrm{PRF}} + n f_{\mathrm{PRF}}$, n is an integer. However, this is not sufficient definition for that since it also depends on the phase of the modulation compared to PRF; AM has no effect even if aforementioned relation holds if pulses occurs at the zero-crossings of AM. Thus, simulating the AM random initial phase should be used. When AM frequency is high compared to PRF and phase is random, or AM frequency slightly differs, however, that the effect of AM is random-like, the MTI can be expect to be quite linearly dependent on the modulation index. High modulation indices show no practical importance but are used for demonstrational purpose.

In Figure 5.12 MTI attenuation is in a function of modulation index with AM frequency of 1 kHz. Frequency is very low compared to the f_{PRF} of 250 kHz and hence the amplitude variation between consecutive pulses is small. This leads to a high attenuation and also small variations between successive simulations. Modulation decreases the attenuation but not significantly due to the very slow AM frequency.

In Figure 5.13 the AM frequency is 10 kHz. Attenuation decreases since amplitude variations are faster. Lowering the PRF would have the same effect because the ratio of the two matters. The variation between simulations increases but the maximum attenuation does not change. Variation between two consecutive pulses depends on

the phase of the modulating sine wave. On the crests and troughs of the wave the derivative is the smallest leading to highest attenuation. Near zero-crossings of the modulating wave the amplitude variation between consecutive pulses is the largest resulting in the smallest attenuation. Thus, the highest attenuation is the same in figures (the lowest points are at the same level) but the variation increases and smallest attenuation decreases due to the larger derivative of higher frequency of the modulating wave.

Noise in reference affects MTI by causing random variations in pulses. MTI in functions of Gaussian amplitude and phase noise and uniform amplitude and phase noise is shown in Figures 5.14a–5.15b. The amount of variations depends on the variance of the gaussian noise or the limiting values of the uniform noise. However, analyzing the effects of noise in more detail requires several issues to be taken into consideration. First of all, amplitude and phase noise are seen differently in the resultant real signal. Secondly, wide bandwidth noise is added to the reference, but the signal goes through filters in the receiver which filter most of the noise out. Thus, not much conclusions can be made based on these constricted tests. However, it is obvious that both amplitude and phase noise behave similarly and the relationship between the amount of noise and MTI is rather linear.

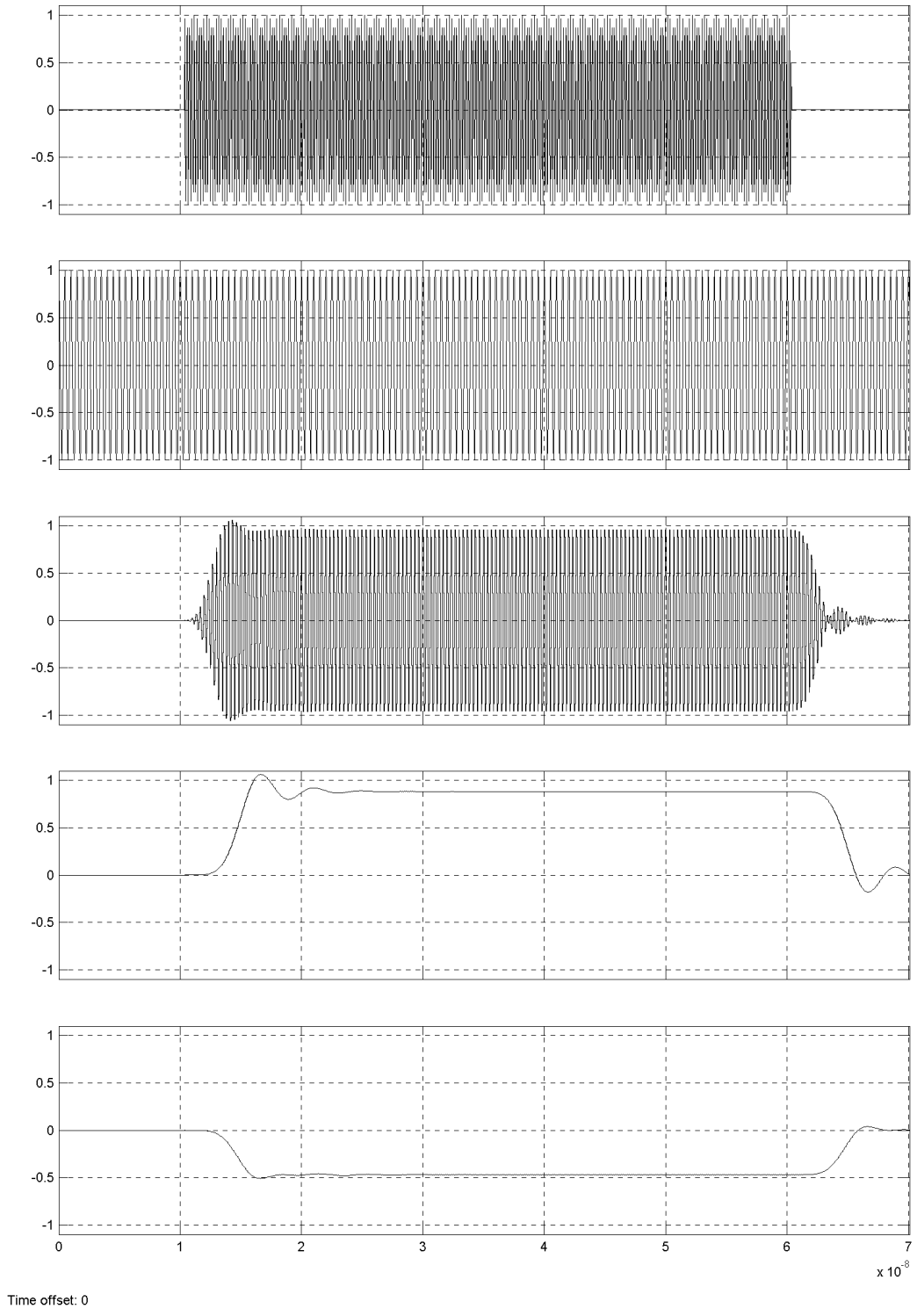

Figure 5.10: *Signals in downmixing and detection. Signal names are from Figure 4.1. From top to bottom: RF-pulse (output y of Propagation and target model block), IF-reference (output if ref r of Signal generator), variable reference (output out of Propagation delay 2), downmixed pulse at IF (output out r of Downmix), and detected pulse at baseband (output out c of IQ-detector).*

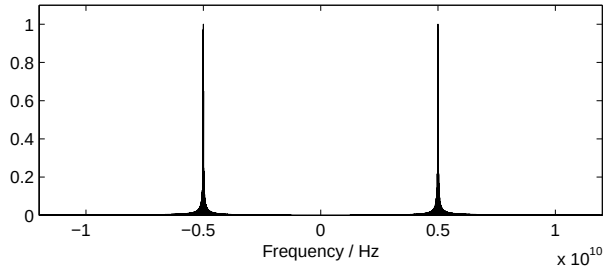

(a) *RF-pulse (output y of Propagation and target model block).*

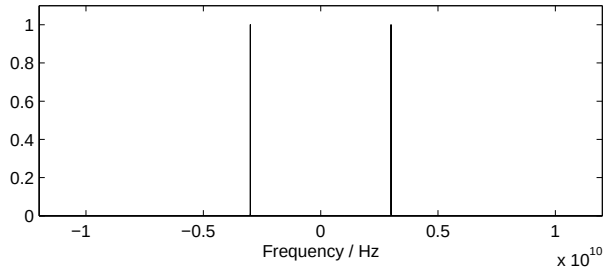

(b) *IF-reference (output if ref r of Signal generator).*

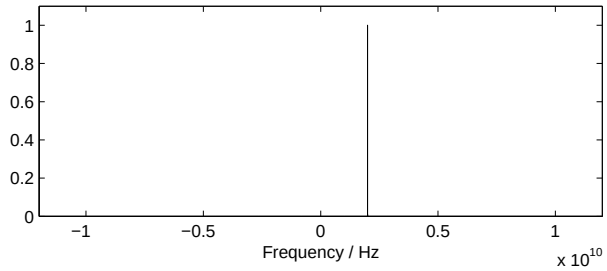

(c) *Variable reference (output out of Propagation delay 2).*

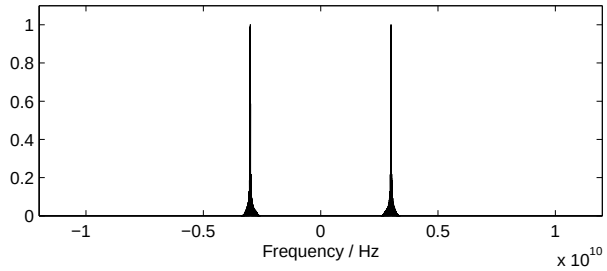

(d) *Downmixed pulse at IF (output out r of Downmix).*

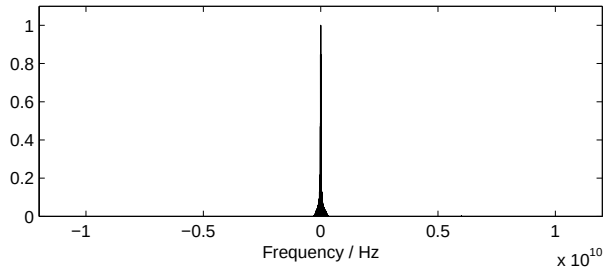

(e) *Detected pulse at baseband (output out c of IQ-detector).*

Figure 5.11: *Frequency spectrums of the signals in Figure 5.10.*

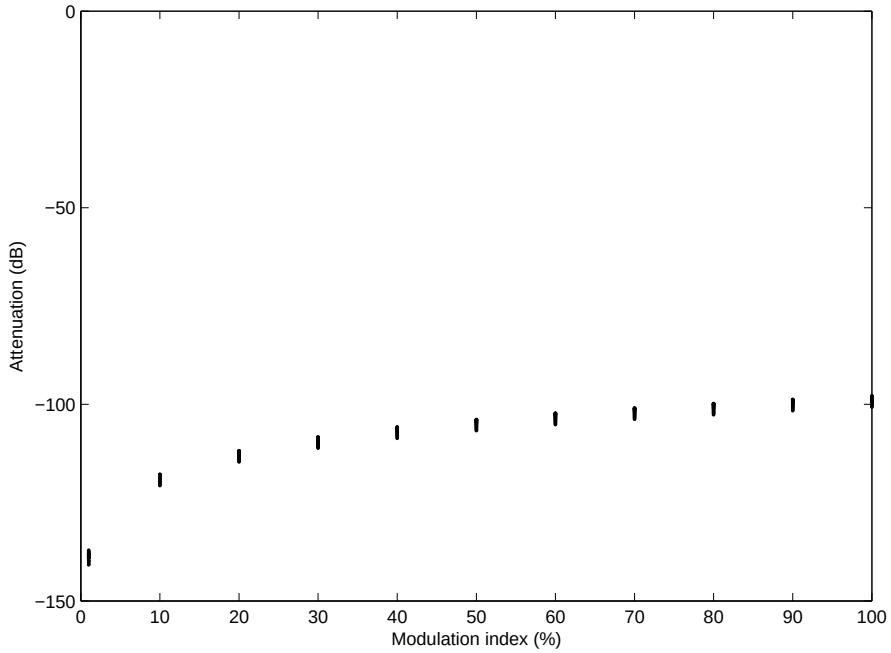

Figure 5.12: *Attenuation in a function of AM index. AM frequency is 1 kHz.*

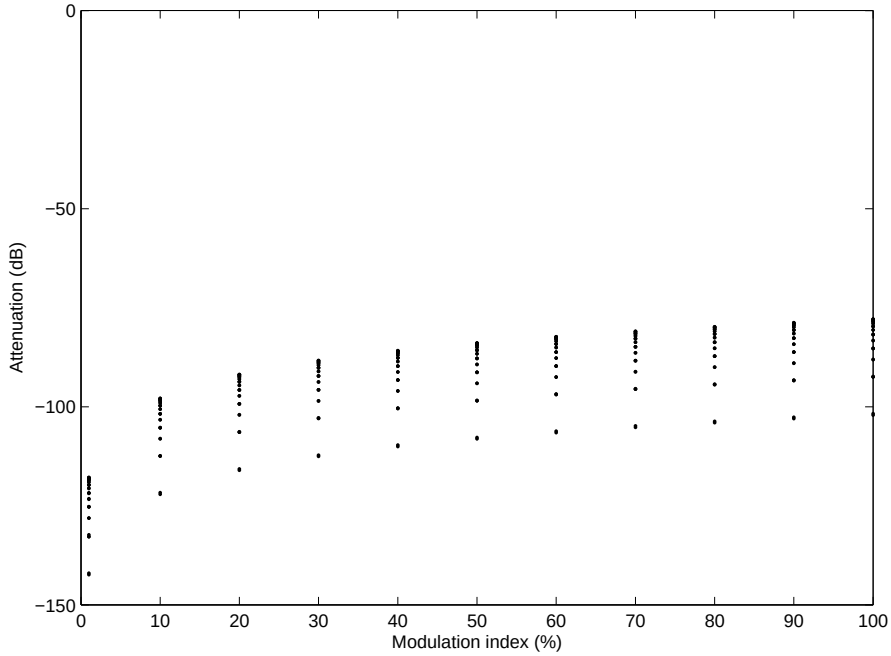

Figure 5.13: *Attenuation in a function of AM index. AM frequency is 10 kHz.*

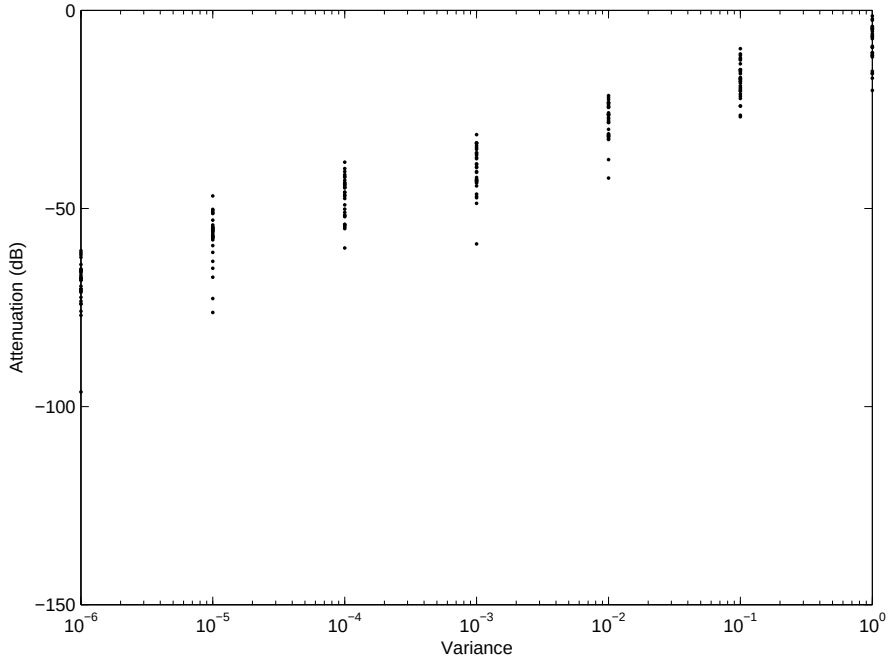

(a) *Gaussian noise variance.*

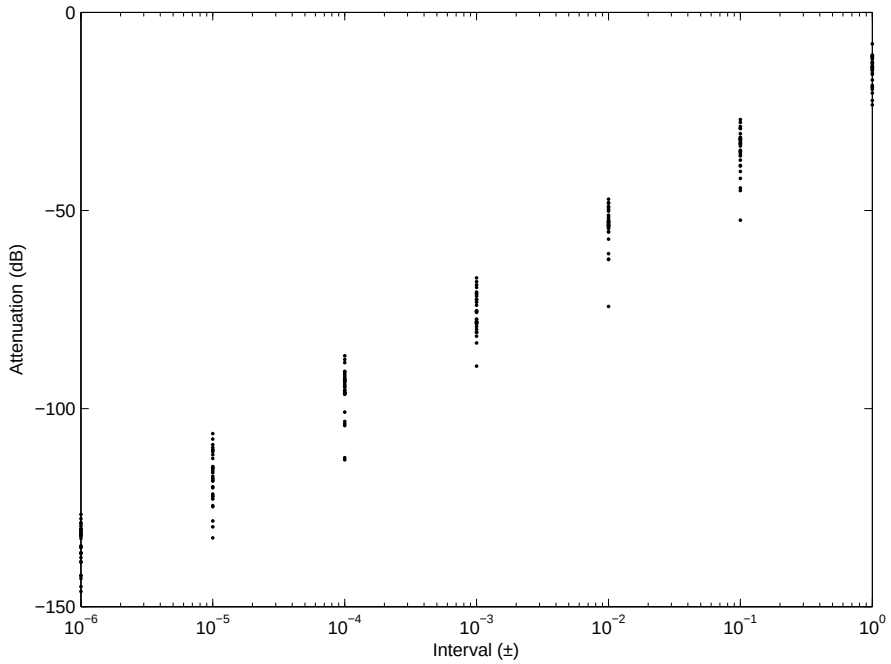

(b) *Uniform noise interval.*

Figure 5.14: *Amplitude noise; attenuation in functions of Gaussian noise variance and uniform noise interval.*

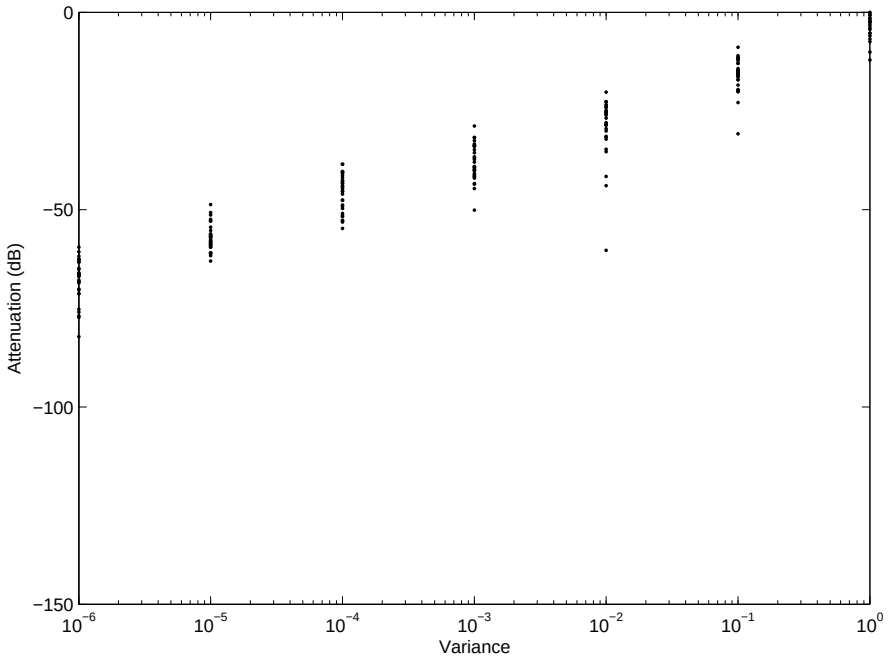

(a) *Gaussian noise variance.*

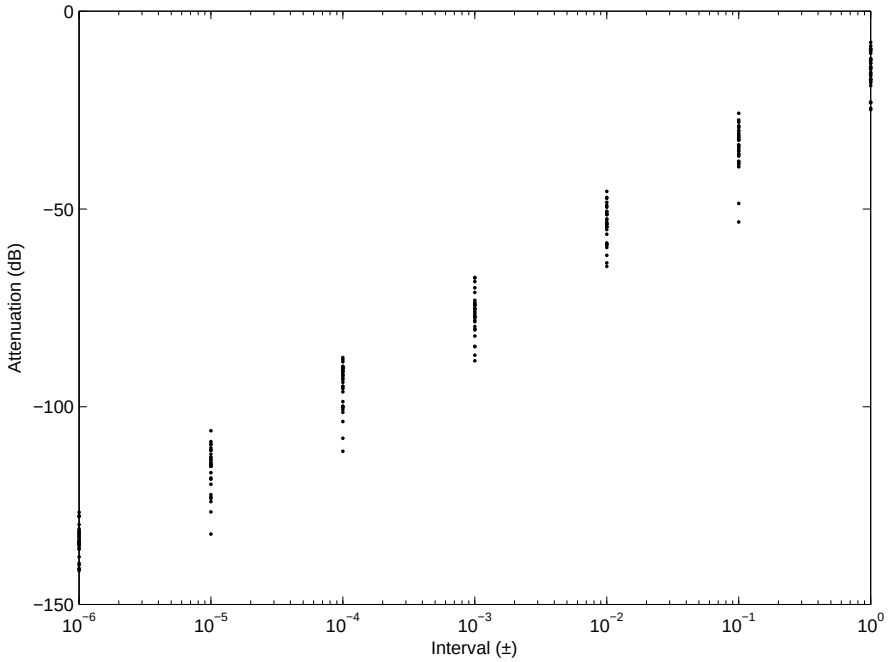

(b) *Uniform noise interval.*

Figure 5.15: *Phase noise; attenuation in functions of Gaussian noise variance and uniform noise interval.*

6. DISCUSSION AND CONCLUSIONS

The initial objective of the study was to analyze the means of synchronization for multistatic radar and examine how they affect the detection probability or end radar image, hence attaining better knowledge of the synchronization and comparing different possible implementations and eventually even find an applicable solution for a real device. However, after a brief literature survey and few meetings with experts of the field, certain synchronization approaches were defined and the conclusion was that a reliable simulation tool was needed to rise to the challenge of analyzing the approaches. Thereby, the work was refocused on the development of the simulation tool to allow analyzing various interferences and errors in radar systems, especially in the path of reference signals needed for the synchronization.

The tool has been implemented using illustrative MATLAB/Simulink which is commonly known and has a modular structure, thus it is easy to modify, improve, and expand for more accurate simulation models and more comprehensive overall simulations. So far it contains the basic structure of radar based on the theory introduced in Chapter 3. The focus has been on the oscillator and timing of radar, especially from the multistatic point of view. Radar needs accurate timing for range measurement and stable phase-coherent operation for Doppler processing. In conventional monostatic radar the same oscillator can be used for transmitter and receiver since they are located at the same site. In this scheme slower drifts and fluctuations in the oscillator are canceled and the high stability is typically required for the propagation time of a pulse. In a multistatic setup two oscillators are needed or the reference signals need to be transferred between the sites. In the case of separate clock oscillators the errors and fluctuations can be additive setting higher accuracy requirements, so at least some periodical synchronization is needed since present clocks are not accurate enough [25, 4] to operate independently. When the synchronization signals are transferred to the reception site, the propagation path has its own effect on the signal, although slower fluctuations may cancel out.

In the implemented simulation tool two reference signals are transferred from the transmitter to the receiver; intermediate frequency reference and variable frequency reference both used directly at the reception. Based on the meetings, the decision was made to model the interferences for now in the variable reference propagation path to keep the overall system simpler and the amount of variables smaller, how-

ever, the interference blocks can be just copied to the IF-reference as well if needed. Possible forms of interference are noise with different characteristics, and amplitude modulation and frequency modulation. These types were partly chosen based on the literature survey on optical fiber transmission [16] which is one possible mean for synchronization signal transfer, and on the meetings. Another mean of interest of examination is direct radio signal transfer. These different means can be analyzed using the simulation tool, when the properties of the propagation path are known, and investigate if they fulfill the stability requirements. Finally some relation between the interferences and detection probability or radar image quality can be derived.

Another implemented feature is a versatile mean of modeling objects. A group of point scatterers are used as a target. The location and RCS of a single point in a function of time is given as a matrix so that the matrices of all points form a target. The matrices are processed before the simulation to imitate an object of interest by moving the points and varying RCS accordingly. The simulator simply calculates the superposition of the responses of all points. The method allows to use complex targets if necessary pre-processing of the target matrix is done.

Despite the very promising platform for real-life imitating simulations is achieved, considerable amount of work is still needed to reliably analyze the performance of a radar or a synchronization mean. Most parts in the simulation are modeled as ideal components so they do not correspond practical components. To modify comprehensive simulation environment the blocks and propagation paths need to be modified to contain at least typical characteristics and errors for those parts and verify the operation comparing to literature or preferably to real devices. This requires time but it can lead to very comprehensive, flexible, and reliable simulation system. Most of the even accurately modeled errors end up being only noise at the end, however, in that way it would be possible to analyze what parts and what errors are significant for the system performance. Thus, it can help aiding where resources should be concentrated if real device is to be developed based on the simulations, this time offering significant savings of time and money. Although the component characteristics are not modeled yet, they have been introduced and their significance assessed in this thesis.

One application of interest to be modeled using the simulation tool is the inverse synthetic aperture radar (ISAR). In ISAR simulation, a target is rotated with typically constant rate and IQ-data is gathered using a high-bandwidth waveform. The data is then ISAR-processed to provide high azimuth resolution and then range-compressed for high-resolution downrange profile. The result can be compared to the measurement performed using a real imaging test radar. After the validation and verification of the simulation tool and the data, interference can be fed to the

reference signals, and hence analyze the effects on the ISAR-image and reflect to the real device.

After getting deeper in the research the goals had to be changed. Getting reliable results for the decision of synchronization method is a challenging task and the topic very broad if comprehensive low-level understanding and simulations are desired. Within the study more knowledge regarding the problem was gathered. A major outcome of the study is the simulation tool itself which can be very valuable tool after more work has been done, based on the mentioned characteristics the simulation lacks. Although absolute performance figures cannot be achieved, some comparison can be done already. Various test simulations have been carried out to validate the functionality of the simulation tool so far. Several figures of the signals were provided to present the operation. The concept of moving target indication has been used to examine the sensitivity of the reference signals to interferences. The results show first proof of the analysis concept for the multistatic radar synchronization. Analytical relation between the reference interferences and the detection probability in surveillance radar or image quality in imaging radar cannot be yet derived. Unfortunately, also the comparison of the simulation results to the real experimental radar was not possible so far. The desire and interest to perform the aforementioned shortcomings still exist, as also does the interest to continue developing the simulation tool based on the promising prospects.

BIBLIOGRAPHY

[1] Baker, B. A Glossary of Analog-to-Digital Specifications and Performance Characteristics. *Texas Instruments Application Report SBAA147B*, October 2011. 33 p.

[2] Brandwood, D. Fourier Transforms in Radar and Signal Processing. Artech House Inc., Norwood, MA, USA, 2003. pp. 58-62.

[3] Blinchikoff, H. J., Zverev, A. I. Filtering in the Time and Frequency Domains. SciTech Publishing Inc., Raleigh, NC, USA, 2006. 520 p.

[4] Eineder, M. Oscillator Clock Drift Compensation in Bistatic Interferometric SAR. IEEE, 2003.

[5] Franco, S. Design with operational amplifiers and analog integrated circuits, 3rd edition. McGraw-Hill Companies, New York, NY, USA, 2002. 672 p.

[6] Garmatyuk, D. High-resolution radar system modeling with MATLAB/SIMULINK. *Defence Electronics*, August 2006, p.12-19.

[7] James, G. Advanced Modern Engineering Mathematics, 3rd edition. Pearson Education Limited, England, 2004. pp. 344-418.

[8] Klemola, O., Lehto, A. Tutkatekniikka, 2nd edition. Otatieto Oy, Helsinki, Finland, 1999. 275 p.

[9] Levanon, N., Mozeson, E. *Radar Signals*, John Wiley & Sons Inc, Hoboken, New Jersey, USA, 2004. 432 p.

[10] McClaning, K., Vito, T. Radio receiver design, SciTech Publishing Inc., Raleigh, NC, USA, 2000. 778 p.

[11] Morris, G., Harkness, L. Airborne pulsed Doppler radar, 2nd edition. Artech House Inc., Norwood, MA, USA, 1996. 510 p.

[12] Nilsson, J. W., Riedel, S. A. Electric circuits, 5th edition. Addison-Wesley Publishing Company Inc., USA, 1996. 992 p.

[13] Nyquist, H. Certain topics in telegraph transmission theory. Transactions of AIEE, vol. 47, pp. 617-644, April 1928. Reprint as classic paper in Proceedings of IEEE, Vol. 90, No. 2, February 2002.

[14] Puranen, M., Eskelinen, P. Measurement of short-term frequency stability of controlled oscillators. Proceedings of the 20th European Frequency and Time Forum, Braunschweig, Germany, pp. 76-79, 2006.

[15] Puranen, M., Eskelinen, P. Improved methods for frequency measurement of short radar pulses. Proceedings of the 21st European Frequency and Time Forum, Geneva, Switzerland, pp. 970-973, 2007.

[16] Romeiser, M. Optical Fibers and RF: A Natural Combination. Noble Publishing, USA, 2004. 271 p.

[17] Rutman, J. Characterization of Frequency Stability in Precision Frequency Sources. Proceedings of the IEEE, vol. 79, no. 6, June 1991.

[18] Shannon, C. E. Communication in the presence of noise. Proceedings of the Institute of Radio Engineers, vol. 37, no. 1, pp. 10-21, January 1949. Reprint as classic paper in Proceedings of IEEE, vol. 86, no. 2, February 1998.

[19] Skolnik, M. I. Introduction to radar systems, 3rd edition. McGraw-Hill Companies, New York, NY, USA, 2001. 772 p.

[20] Skolnik, M. I. Radar handbook, 3rd edition. McGraw-Hill Companies, New York, NY, USA, 2001. 1299 p.

[21] Stimson, G. Introduction to Airborne Radar, 2nd edition. SciTech Publishing Inc., Mendham, New Jersey, USA, 1998. 584 p.

[22] Tian, W., Liu, H., Zeng, T. Frequency and Time Synchronization Error Analysis Based on Generalized Signal Model for Bistatic Radar. IEEE.

[23] Willis, N. J. Bistatic radar, 2nd edition. SciTech Publishing Inc., Raleigh, NC, USA, 2005. 329 p.

[24] Wehner, D. R. High-Resolution Radar, 2nd edition. Artech House Inc., Norwood, MA, USA, 1987. 616 p.

[25] Yongsheng, Z., Diannong, L., Zheng, D. Analysis of Time and Frequency Synchronization Errors in Spaceborne Parasitic InSAR System. IEEE, 2006.

[26] Young, H. D., Freedman, R. A. University physics with modern physics, 11th edition. Addison-Wesley Publishing Company Inc., USA, 2003. 1714 p.

[27] Ziomek, C., Corredoura, P. Digital I/Q Demodulator. Proceedings of the 1995 IEEE Particle Acceleration Conference, p.2663-2665.

[28] Wang, W-Q. GPS-Based Time & Phase Synchronization Processing for Distributed SAR. IEEE Transactions on Aerospace and Electronic Systems, vol. 45, no. 3, July 2009.